Geophysical Journal (1989) **96**, 497–517

Late Pleistocene and Holocene sea-level change in the Australian region and mantle rheology

Masao Nakada* and Kurt Lambeck

Research School of Earth Sciences, The Australian National University, Canberra, ACT 2601, *Australia*

Accepted 1988 September 14. Received 1988 September 9; in original form 1988 May 26.

SUMMARY

Spatial and temporal variations in sea-level are produced by the melting of the Late Pleistocene ice and by the Earth's response to the redistribution in surface loads. By examining different parts of the sea-level curves of the past 20 000 yr from geographically widely distributed regions it becomes possible to constrain models of the melting history of the ice sheets and of the Earth's rheology. Observations from sites away from the former Arctic ice sheets, such as the Australian and South Pacific region, are particularly important for constraining the total meltwater volumes added into the oceans in the past 20 000 yr and the rates at which this occurred. These observations indicate that the Antarctic ice sheets provided a significant contribution to the sea-level rise at a rate that was approximately synchronous with the melting of the Laurentide ice sheet, except for the interval 9000–6000 yr ago when it may have lagged behind. Minor melting of the Antarctic ice sheet appears to have continued throughout the Late Holocene. Differential observations of the Late Holocene sea-level change recorded at sites in the same region are particularly useful for estimating parameters describing the Earth's non-elastic response to surface loading. The effective parameters used here are a lithospheric thickness, an upper mantle viscosity, and a lower mantle viscosity describing the response below 670 km depth. With the observations used here, it is not possible to separate the lithospheric thickness H from the upper mantle viscosity and the viscosity results are based on the assumption that $50 \lesssim H \lesssim 100$ km. Neither do these observations provide a resolution of the depth dependence of viscosity in the upper mantle and the resulting estimates are effective parameters only. Differential sea-levels along continental margins and along the shores of large gulfs and bays constrain the effective upper mantle viscosity to be about $(1\text{–}2) \times 10^{20}$ Pa s^{-1} while differential values from islands of different sizes are suggestive of a somewhat lower value. The lower mantle (taken to be below 670 km depth) viscosity is about two orders of magnitude greater than this. The estimated ice and rheological models explain many of the Holocene sea-level observations throughout the Australian and southern Pacific region. The tilting of continental margins, as exemplified by observations of variable amplitudes of the Holocene high-stands and the variable times at which sea-levels first reached their present level along the north Queensland coast and Great Barrier Reef, is well represented by these models. Differential Holocene sea-levels observed along the narrow Spencers Gulf of South Australia are also well explained by the models and in neither case is it necessary to invoke tectonic motions. Predicted Late Holocene sea-levels at small- to medium-sized islands are characterized by small amplitude high-stands that reached their maximum values about 4000–2000 yr ago, consistent with observations from the Society, Cook and Tuamotu Islands.

Key words: ice sheet melting models, mantle rheology, sea-level, vertical tectonics

INTRODUCTION

Observations of Late Pleistocene and Holocene sea-level variations are important for studying the tectonic histories of continental margins and ocean islands, for evaluating the mechanical response of the Earth to surface loading, and for constraining the melting histories of the large polar ice sheets. A separation of the parameters that define these various processes is possible in principle by examining records of sea-level change over different time periods from geographically widespread sites. For example, sea-level change at sites near the former ice load (locations in the near-field) exhibit a quite different dependence on the various parameters defining the Earth's response and the ice load's geometry through space and time than do sea-level changes at sites far from the ice sheets (the far-field). For

* Now at the Faculty of Science, Kumamoto University, Kumamoto, Japan.

the far-field sites, the sea-level variations before about 6000 yr ago are relatively insensitive to the parameters defining the Earth's response to time-dependent surface loading whereas the mid- to late-Holocene part of the curve is more sensitive to this response (see, for example, Farrell & Clark 1976; Peltier & Andrews 1976).

Sea-levels in the near-field, where the changes are most dramatic, particularly at locations in eastern Canada and along the Atlantic coast of North America, have been extensively used to estimate the rheological structure of the Earth's mantle (e.g. Cathles 1975; Wu & Peltier 1983; Sabadini, Yuen & Gasperini 1985; Yuen *et al.* 1986). But the changes at such sites, close to the margins of the Late Pleistocene ice sheets, are about equally sensitive to the rheology of the mantle as to the detailed description of the ice load and generally the latter is inadequately known for the purpose of estimating the Earth's viscosity (e.g. Nakada & Lambeck 1987, 1988a). Furthermore, the sea-level changes here may also indicate tectonic movements caused by the sediment loading of the glacial outwash associated with the disintegration of the ice sheets (e.g. Newman *et al.* 1980). We therefore avoid using these data here and instead focus on sea-level observations in the far-field, at sites that lie at a considerable distance from both the Arctic and Antarctic ice sheets.

Sea-level change in the far-field is characterized by a rapid rise during the melting phase from about 18 000 yr before present (yr BP) to about 6000 yr BP and a nearly constant level from about 6000 yr BP to the present. These changes are predominantly indicative of the rates at which the meltwater has been added into the oceans. Regional variations from this general pattern occur because of the response of the Earth to the time-dependent meltwater and ice loads as the ice mass is transferred to the oceans. This was recognized by Bloom (1967), Walcott (1972) and Chappell (1974) who attempted to estimate mantle viscosity from observations of regional variations in the sea-level curve. The first global analyses of the far-field sea-levels were by Cathles (1975), Farrell & Clark (1976) and Clark, Farrell & Peltier (1978) and these studies have indicated that such data for tectonically stable regions can be used to constrain both the rheological structure of the mantle and the gross melting characteristics of the ice sheets (see also Nakiboglu, Lambeck & Aharon 1983; Nakada & Lambeck 1988b).

FAR-FIELD OBSERVATIONS OF HOLOCENE SEA-LEVEL CHANGE

The sea-levels examined in this paper are from the Australian and New Zealand region and from a few selected SW Pacific sites. This choice may seem parochial but it is guided by the Australian continent being tectonically stable over this time interval and by the careful fieldwork done in this area. Few other far-field regions meet these conditions. Following upon the pioneering paper by Fairbridge (1961), much detailed work has been carried out in the Australasian region and the results for Australia have been summarized by Hopley & Thom (1983), Hopley (1987) and Chappell (1987), while the New Zealand evidence has been summarized by Gibb (1986). The Australian region, generally far from plate boundaries and free from significant Quaternary tectonics, is believed to be relatively stable. New Zealand provides a less stable platform for measuring sea-level changes, although the eastern edge of the South Island, south of about Christchurch, and the NW area, near Auckland, is believed to be relatively stable (Wellman 1979). Ocean islands, particularly young islands, are prone to tectonic subsidence but sea-levels from these sites are important in that, when compared with continental margin observations, they may provide evidence for lateral variations in the Earth's response to surface loading. Recent observations include those by Pirazzoli *et al.* (1985, 1987) and Pirazzoli & Montaggioni (1984) for the Tuamotu and Society Islands.

The principal diagnostic characteristics of the sea-level curves observed at these far-field regions are (i) the amplitudes of sea-level, relative to the present level, at about 6000 yr BP, (ii) the time when sea-level reached its present level or obtained its maximum Holocene level, (iii) the rates of sea-level rise from about 10 000 to 6000 yr BP, and (iv) the sea-level at about 18 000–20 000 yr BP. The records prior to about 6000 yr BP in these regions are primarily indicative of the gross melting characteristics of the ice sheets; of the total volume of meltwater that has been added to the oceans and of the rates at which this meltwater has been added (Nakada & Lambeck 1988b).

Figure 1 summarizes the Australian observations of the position of sea-level, relative to the present level, at about 6000 yr BP where these Holocene high-stands have been identified (see papers in Hopley 1983a, b; Chappell 1987). The occurrence of these high-stands is in the range 5000–6000 yr BP (Table 1). Also indicated are locations where the high-stand has not been clearly identified but where this level is believed to be close to the present sea-level. The best information is from Karumba, in the Gulf of Carpentaria, the Great Barrier Reef of northern Queensland (typified by the Halifax Bay site), the coast of New South Wales (typified by the Moruya site), and Spencer Gulf, South Australia. Information from the other sites are usually restricted to isolated observations whose reliabilities are difficult to assess. Several regional patterns can be seen in these observations. Well defined Holocene high-stands are found along the NE coast from the Gulf of Carpentaria to as far south as central Queensland with amplitudes ranging from 0.5 to 3 m above present levels. Along this coastline Holocene sea-levels for offshore islands are generally lower than those observed at the continental margin. The Holocene high-stand has not been clearly identified along the coast of New South Wales and Thom & Roy (1983, 1985) concluded that this level did not exceed 1.0 m above present sea-level (see also Hopley 1987). Nor have Holocene high-stands been found along the coast of Tasmania either. An extensive study of the South Alligator River estuary in the Northern Territory failed to find evidence for a Holocene high-stand (Woodroffe *et al.* 1987) but tentative identifications have been made further to the west within the estuaries of the Ord and Fitzroy Rivers of Western Australia (Brown 1983). The sea-level observations along the west coast of Australia have been reviewed by Brown (1983) and estimates of maximum Holocene levels range from about 0.5 to 3 m above their present levels. The lower value corresponds to a site in the Swan River Estuary near Perth (Kendrick 1977) whereas the higher value

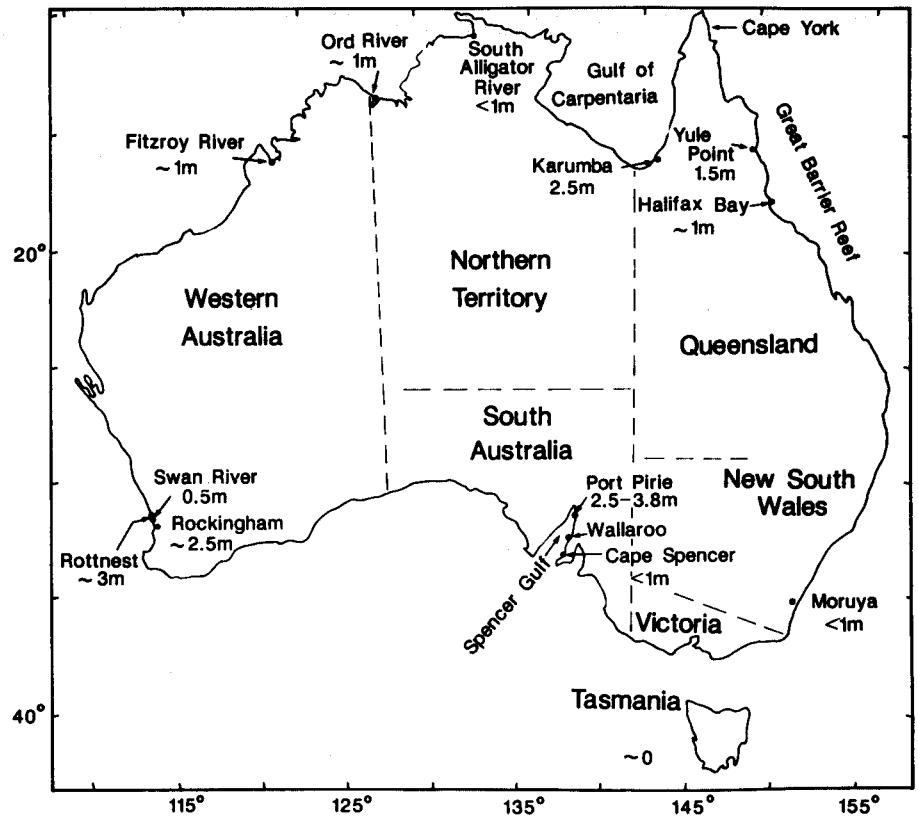

Figure 1. Location map and amplitudes of some Late Holocene sea-level high-stands observed around the Australian coastline (see Table 1 for details).

corresponds to sites on Rottnest Island, about 20 km offshore (Playford 1983), and to sites north and south of Perth (Woods & Searle 1983; Searle & Woods 1986). The differences between these and the Swan River result are, as emphasized by Chappell (1987), hard to reconcile unless there has been some local tectonic movement (Playford & Leech 1977). Clear Holocene high-stands have been identified in the Spencer Gulf, along the southern margin of the continent, where the highest levels of 2.5–3.8 m occur at the head of the gulf near Port Pirie (Burne 1982; Belperio *et al.* 1984; Hails, Belperio & Gostin 1984) but there is no clear evidence for Holocene high-stands at the entrance to the gulf (Belperio, Hails & Gostin 1983).

Table 1. Holocene high-stand amplitude and time of occurrence for selected sites in Australia and New Zealand (see Fig. 1).

Site	ζ max (m)	Time (kyr BP)	Reference
Karumba	~2.5	6.0	Chappell *et al.* (1982)
Halifax Bay	1.0–1.5	6.0	Chappell *et al.* (1983)
New South Wales	0.0–1.0	~6.0	Thom & Roy (1983, 1985)
Port Pirie	2.5–3.8	~6.0	Burne (1982), Belperio *et al.* (1984), Hails *et al.* (1984)
Cape Spencer	~0.0		Belperio *et al.* (1983)
Rottnest Island	3.0	5.5–6.0	Playford (1983)
Swan River estuary	0.5	~5.0	Kenrick (1977)
Alligator River	<1.0		Woodroffe *et al.* (1987)
Tasmania	~0.0		Hopley (1987)
Christchurch	0.9	~6.5	Gibb (1986)
Auckland (Hauraki Gulf)	<1.0	~6.3	Gibb (1986)

The Holocene sea-level observations for New Zealand at three different locations where tectonic movements are believed to have been negligible (Auckland, Christchurch and Blueskin Bay near Dunedin) are indicative of an almost constant sea-level from the time, at about 6500 yr BP, when the sea surface first reached its present level and Holocene maxima above present level have not exceeded 1 m (Gibb 1986). For the Pacific islands of the southern Cook, Tuamotu and Society groups, this level is not always evident but where it is, it was generally reached later than 600 yr BP and the maximum Holocene high-stands have been variously dated at between 4000 and 2000 yr BP (Fig. 2). The evidence for this includes micro-atolls (Stoddart, Spencer & Scoffin 1985; Yonekura *et al.* 1984), the ages of cementation of reef debris, and the ages of chemical alteration of the cements (Pirazzoli *et al.* 1985).

THE SEA-LEVEL EQUATION

The equation describing the sea-level variation, ζ, caused by the transfer of mass between the ice sheets and oceans on a viscoelastic Earth has been formulated by Farrell & Clark (1976). The solution for the relative sea-level (RSL), defined as

$$\Delta\zeta(\theta, \lambda; t) = \zeta(\theta, \lambda; t) - \zeta(\theta, \lambda; t_0) \quad (1)$$

at colatitude θ, longitude λ and time t, can be written as

$$\Delta\zeta(\theta, \lambda; t) = \Delta\zeta_R(\theta, \lambda; t) + \Delta Z_1(\theta, \lambda; t) + \Delta Z_2(\theta, \lambda; t) \quad (2)$$

(Nakada & Lambeck 1987), where t_0 is the present time.

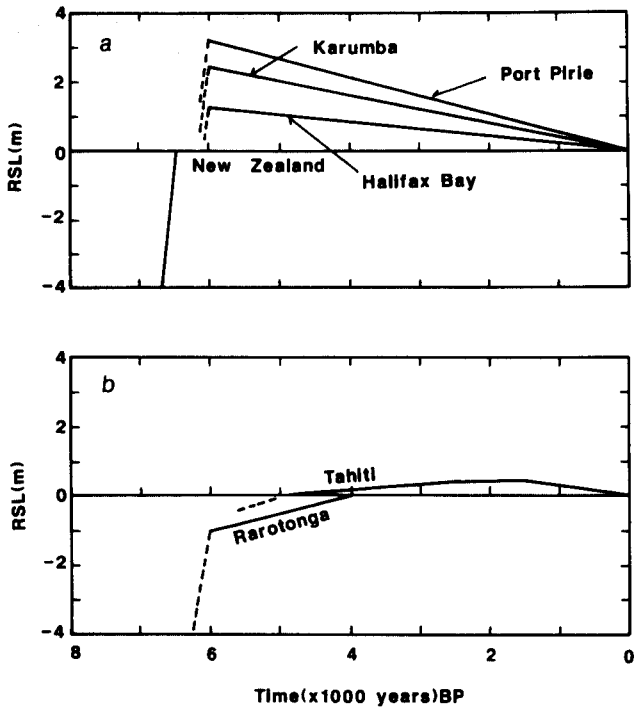

Figure 2. Schematic relative sea-level curves (RSL) with respect to present-day values observed at selected sites in (a) Australia and New Zealand and (b) the South Pacific.

Here $\Delta\zeta_R$ is the relative sea-level variation on a rigid Earth and includes the equivalent sea-level change defined as

$$\frac{\text{(meltwater volume at time } t) \times \text{(ice density)}}{\text{(area of ocean surface)} \times \text{(seawater density)}}, \quad (3)$$

and the gravitational terms defining the attraction between the ice sheets and oceans. This term can be neglected for the post-glacial phase; for the times when no further meltwater is added to the ocean. The other two terms in equation (2), ΔZ_1 and ΔZ_2, allow for the deformation of the Earth in response to the change in the ice and water load. ΔZ_1 represents the sea-level change produced by the deformation associated with the changes in ice load volume and includes the modifications produced by self-attraction and the Earth's viscoelastic deformation as a result of this surface load. The term ΔZ_2 represents the sea-level change associated with the deformation produced by the meltwater loading and includes the associated self-attraction and Earth deformation. The two terms are defined such that mass is conserved and the ocean surface is an equipotential at all times. Details for the definition of these terms are given by Nakada & Lambeck (1987). To obtain quantitative solutions of the sea-level equation, the required inputs are (i) the spatial and temporal description of the ice model, (ii) a geometric description of the ocean surface, and (iii) a rheological model of the Earth.

Ice model

The details of the melting histories of the polar ice sheets, both the geographical distribution and the rates of melting, are most important for understanding the sea-level changes at sites near the margins of the ice sheets and the uncertainties in these ice models are generally such that it is not possible to draw realistic conclusions about the Earth's response from data collected at such sites. These details are much less important at the far-field sites considered here where sea-level change is primarily dependent upon the volumes and rates at which the meltwater has been added to the oceans. Three major ice sheets are considered here; (i) the Laurentide and western Cordilleran ice sheet, including the Innuitian and Greenland parts, (ii) the Fennoscandian and Barents–Kara shelf ice sheets, and (iii) the Antarctic ice sheet. The ICE 1 model of Peltier & Andrews (1976), smoothed and defined here with a 1° spatial resolution, has been adopted for the first contribution although, for these far-field evaluations, coarser definitions of the spatial distribution of the ice loads are adequate. Melting of the Laurentide ice sheet is assumed to have been complete by 6000 yr BP. For the second contribution, the Fennoscandian part of the above ICE 1 model has been adopted and this, plus the Laurentide ice model defines the ARC 1 model of Nakada & Lambeck (1987). To this has been added an approximate model of the Barents–Kara ice sheet, based on the maximum model of Denton & Hughes (1981), which has an equivalent sea-level rise of about 12 m and whose rate of melting has been assumed to be synchronous with the equivalent sea-level change of the Fennoscandian ice of ARC 1. The sum of the contributions (i) and (ii) is referred to here as ARC 3 and its sea-level equivalent as defined by (3) is 89 m. Because the Fennoscandian ice sheet vanished by about 10 000 yr BP (De Geer 1954) the detailed time–space distribution of this and the Barents–Kara loads is unimportant in discussions of far-field sea-level change for the past 8000–10 000 yr.

Several descriptions of the Antarctic contribution are used here. The first is the model ANT 1 of Nakada & Lambeck (1987) which is based on the ice sheet reconstruction at 18 000 yr BP by Denton & Hughes (1981, p. 269) and the present ice sheet thicknesses given by Drewry (1982). Each ice column in this sheet has been assumed to melt at the same rate, synchronous with the bulk melting of the Arctic ice sheet ARC 1 (Fig. 3), consistent with the hypothesis that the Antarctic ice sheet disintegrated, with minimal time-lag, in response to the rising sea-level produced by the melting of the northern ice sheet. The contribution of the Antarctic models to the equivalent sea-level rise is about 37 m, greater than the 24 m proposed by Denton & Hughes (1981). A second description, ANT 2, based on the Wu & Peltier (1983) model in which the assumption was made that Antarctic melting preceded Arctic deglaciation, is rejected on the basis of its inconsistency with far-field sea-level observations (Nakada & Lambeck 1987, 1988b; see also Nakiboglu *et al.* 1983).

The maximum sea-level drops in the far-field at about 18 000 yr BP constrain the total meltwater, and observations indicate that this level occurred at between 100 and 150 m below the present level (Table 2). Chappell (1987) has reviewed the evidence for this low-stand in the Australasian region and concludes that these depths are about 130–150 m below present sea-level. Ota, Matsushima & Moriwaki (1981) concluded that around Japan these depths occurred at about 130 m below present sea-level. Some regional variation in this level can be expected because of the Earth's

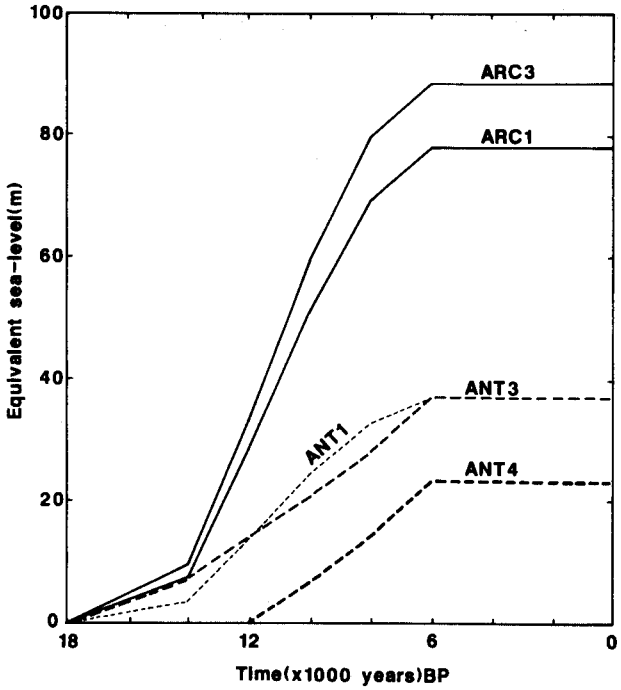

Figure 3. Equivalent sea-level rise (ESL) for two Arctic ice models ARC 1 and ARC 3 and three Antarctic ice models ANT 1, ANT 3, ANT 4.

deformation but this is relatively small for far-field sites and not very sensitive to the choice of mantle model. The ice models ARC 3 and ANT 1 produce low-stands of between about 120 and 140 m for the sites included in Table 2 and are in reasonable agreement with the observed values except that they do not reproduce the values near 150 m depth suggested for some localities.

Nakada & Lambeck (1988b) noted that for the period 10 000 to 6000 yr ago the predicted sea-levels, based on the models ARC 3 + ANT 1, generally rose faster and earlier than observed and they suggested that the Antarctic ice sheet may have melted somewhat later than the Arctic ice sheet. This forms the basis for the equivalent sea-level model ANT 3 illustrated in Fig. 3 and in the following discussions we use the ice models ARC 3 and ANT 3 as the reference ice-load model.

Because of the predicted regional variation in the sea-level response and because of the considerable uncertainty that is associated with the adopted ice model, it

Table 2. Estimates of the lowest stand of sea-level in the far-field at about 20 000 to 18 000 yr ago. The predicted values are based on the ice models ARC 3 + ANT 3 and on a rheological model of $H = 50$ km, $\eta_{um} = 2 \times 10^{20}$ Pa s^{-1}, $\eta_{lm} = 10^{22}$ Pa s^{-1}.

Area	Reference	Observed depth (m)	Predicted depth (m)
North Queensland	Carter & Johnson (1986)	114–133	129
Huon Peninsula	Chappell & Shackleton (1986)	130	126
Central Japan	Ota *et al.* (1981)	~130	122
Timor Sea	van Andel & Veevers (1967)	130	136
Central Queensland	Veeh & Veevers (1970)	150–175	130
Arafura Sea	Jongsma (1970)	150–175	138

is necessary to establish whether the sea-levels in the Australian and Paçific regions are sensitive to the distribution of the load within the ice sheets. Sea-levels in this region are insensitive to the geographical distribution of the northern hemisphere ice sheets (Nakada & Lambeck 1988b) but because of their closer proximity to Antarctica it remains to be demonstrated the degree to which the observations are sensitive to the details of the Antarctic load. Fig. 4 illustrates the thickness of the ice that is assumed to have been removed between 18 000 and 6000 yr BP. To examine the dependence of the Australian and New Zealand sea-levels on details of melting the Antarctic ice sheet has been divided into three sectors, an eastern sector (A) over which little change has occurred and two sectors (B, C), centred on the Ross and Weddell Seas respectively, which are the major sources of meltwater. The equivalent sea-level contributions to the global model ANT 3 from each of these sectors are illustrated in Fig. 5. Each ice column of sector A is assumed to have melted synchronously with the equivalent sea-level model for ANT 3 and two rather extreme hypothetical cases of differential melting times for the sectors B and C have been adopted for which the total equivalent sea-level curve remains unchanged: in the first (Fig. 5b), the available ice in sector B has decayed before melting starts in sector C, and in the second (Fig. 5c) the sequence of hypothetical melting rates has been reversed. The resulting sea-level variations at four sites are illustrated in Fig. 6 and in all cases the differences are small, particularly for the sites furthest from Antarctica. These differences remain small over a range of realistic earth models and the sea-level observations used in this study are not sensitive to details of the geographic distribution of Antarctic ice load.

Ocean function

The geometry of the ocean surface on to which the meltwater is added, is defined by the ocean function, a function that equals 1 where there is ocean and 0 where there is land. The resolution required to describe this function is variable but can be very high for those localities where the mid- to late-Holocene sea-level variation is controlled by the distribution of the meltwater in the vicinity of the point of observation. Past studies of global variations in sea-level used fairly coarse definitions of the ocean function. Nakiboglu *et al.* (1983) used a 10° resolution and Cathles (1975, 1980) and Lambeck & Nakada (1985) used 5°. Wu & Peltier (1983) used a variable resolution of about 5° in the near-field and along some continental margins, and as large as 20° in mid-ocean regions of the far-field. These coarse definitions fail to model the regional response to local loading but, as already demonstrated by Chappell *et al.* (1982), such variations in the Earth's response can be significant over distances much less than 500 km (see also Nakada 1986). Nakada & Lambeck (1987) found that an ocean function described with 10′ spatial resolution and expanded into spherical harmonics up to degree 180 provided an adequate description of the ocean function for all observation sites examined, provided that a lithospheric thickness of not less than about 50 km is adopted. The use of greater thickness lithospheres, by improving the convergence of the solution of the sea-level equation,

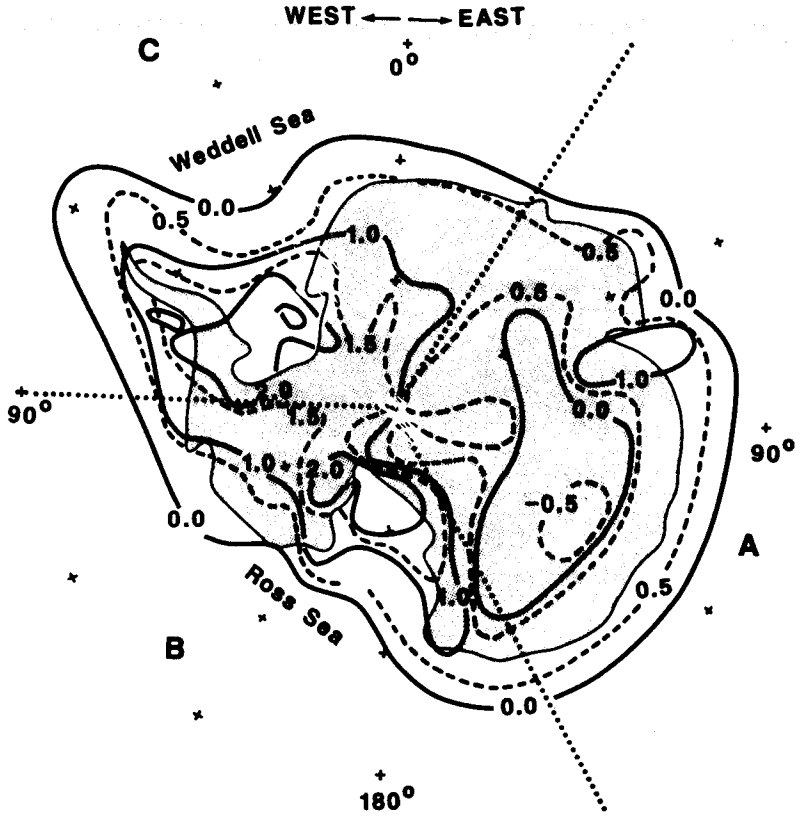

Figure 4. Thickness of Antarctic ice removed between 18 000 and 6000 yr BP (in km).

reduces the need for this high resolution but any estimates of this thickness would then be geophysically meaningless (Nakada & Lambeck 1988a). We use here the 10′ spatial description of the ocean geometry and adopt a lithospheric thickness of 50 km.

Earth models

The Earth's response to surface loading on characteristic time-scales of 10^3–10^4 yr, is represented by a Maxwell viscoelastic body with a depth-dependent Newtonian viscosity. Most of the glacial rebound observations appear to be adequately described by such a model (e.g. Kaula 1980) and there are no compelling observational reasons for adopting a non-linear rheology to describe the rebound phenomena. The rigidity, bulk modulus and density are those of the preliminary earth reference model (PREM) of Dziewonski & Anderson (1981). The lithosphere is assumed to have a viscosity of 10^{25} Pa s^{-1} so that it responds essentially as an elastic layer to loads on time scales of 10^3–10^4 yr. The mantle viscosity is assumed to be two-valued, an upper mantle viscosity η_{um} and a lower mantle viscosity η_{lm} where the boundary between the two regions is taken to correspond to the 670 km discontinuity. Rebound models with asthenospheric low viscosity channels (Walcott 1973; Cathles 1975) have not been explored here in detail but trial calculations with a low viscosity channel of 170 km thickness immediately beneath the lithosphere

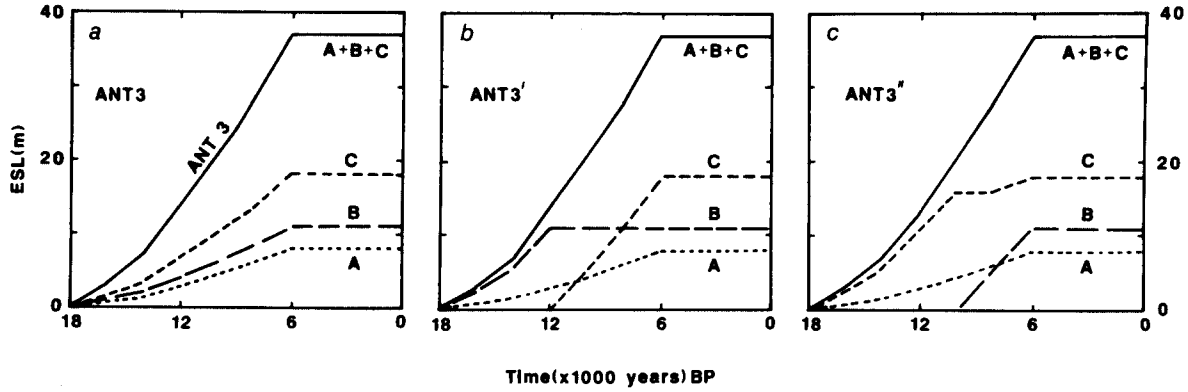

Figure 5. Three schematic models for equivalent sea-level rise resulting from differential rates of melting of the sectors A, B, C of Antarctica defined in Fig. 4.

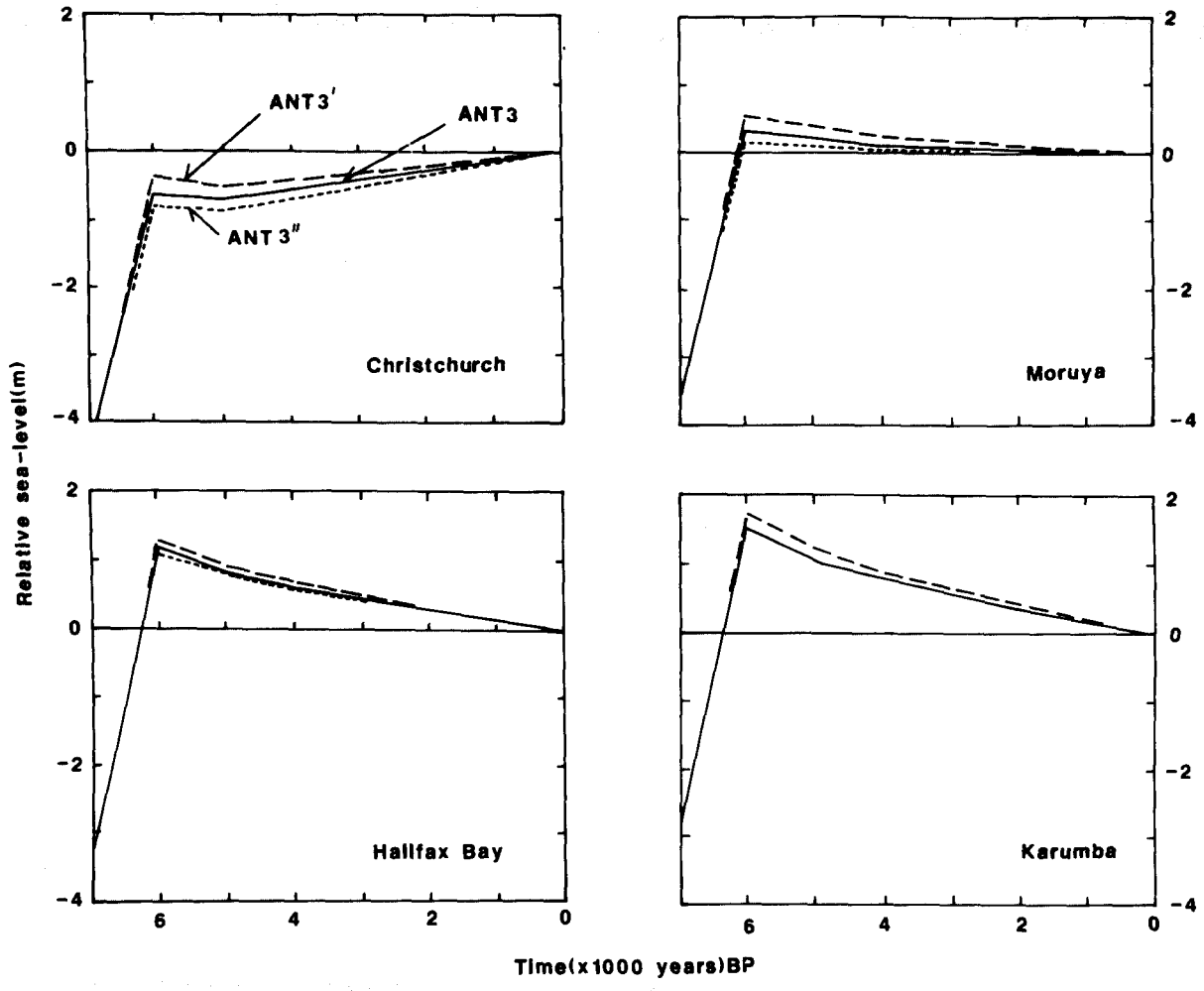

Figure 6. Late Holocene sea-levels relative to present-day levels predicted by the melt models ANT 3 and the two modifications ANT 3′ and ANT 3″ of the Antarctic contribution with (H, η_{um}, $\eta_{lm} = 50$ km, 10^{20} Pa s^{-1}, 10^{22} Pa s^{-1}).

indicate that the sea-level response at most of the far-field sites considered here is not very sensitive to the depth dependence of the viscosity of the upper mantle and that only the average upper mantle viscosity can be resolved. Only at large island sites in the far-field, such as New Zealand or Fiji, does the introduction of a low viscosity channel have a measurable effect but here the separation of viscosity parameters from lithospheric thickness estimates does not appear to be readily possible (see Appendix 1).

The solutions for the response of the viscoelastic body use the correspondence principle and they imply that the body is non-adiabatic (Cathles 1975). Fjeldskaar & Cathles (1984) suggested that this assumption was inappropriate and that, under certain conditions, this could lead to erroneous conclusions being drawn from observations of the response of the Earth to glacial unloading. Approximate calculations, however, have indicated that for far-field sites and for sea-level change during the late- and post-glacial phase the question of whether the mantle is adiabatic or non-adiabatic is not important as can also be seen directly from fig. 9 in Fjeldskaar & Cathles (1984).

THEORETICAL CHARACTERISTICS OF THE HOLOCENE SEA-LEVEL CHANGES

The sea-level changes during the post-glacial period are represented by the sum of the two terms ΔZ_1 and ΔZ_2 (equation 2) representing the deformation of the crust produced by the melting of the ice sheets and by the loading of the ocean crust by the meltwater respectively. These two terms, plus the total relative sea-level change defined by (2), are illustrated in Fig. 7 for the epoch 6000 yr BP for the Australian, New Zealand and Pacific sites discussed previously. In the first instance the lithospheric thickness has been held constant at 50 km and the upper mantle viscosity is assumed to be 10^{21} Pa s^{-1}. The lower mantle viscosity is allowed to vary through two orders of magnitude. The results are characteristic for a range of plausible upper mantle viscosities.

In Fig. 7(a) ΔZ_1 and ΔZ_2 are given for the northern ice models ARC 1 and ARC 3 although the results differ only little from each other. The ΔZ_1 term does not produce differential sea-levels across the region due to the fact that the sites are all located in the far-field of the Arctic ice

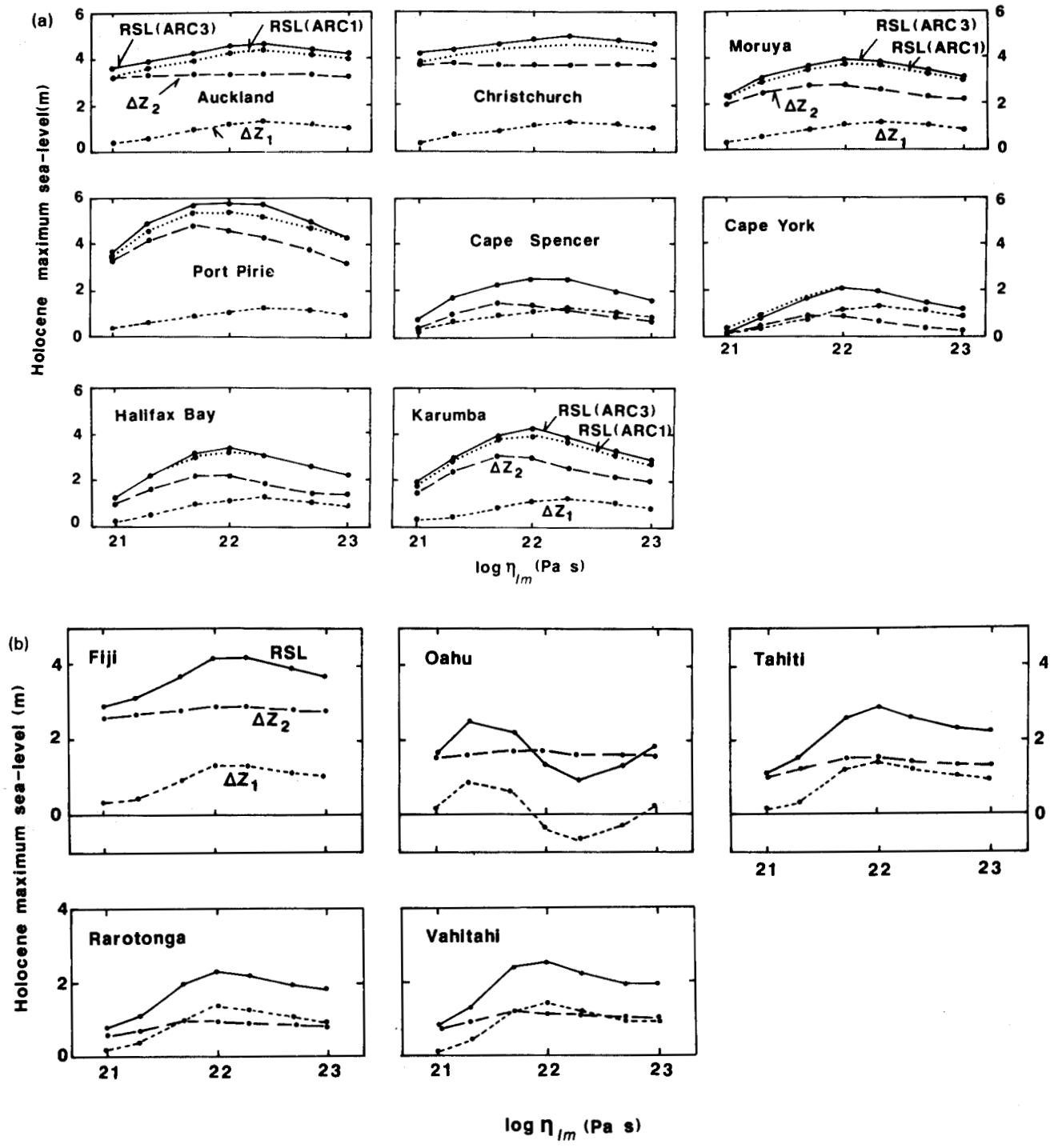

Figure 7. Maximum Late Holocene sea-levels (RSL), the ice unloading term ΔZ_1 and the meltwater loading term ΔZ_2 as a function of lower mantle viscosity. The upper mantle viscosity is 10^{21} Pa s^{-1} and lithospheric thickness is 50 km. (a) For continental margin sites and Arctic ice models, (b) for island sites of different surface areas and Arctic ice models, (c) for continental margin sites and the Antarctic ice model ANT 3.

sheets where the sea-level variations are not sensitive to the details of the ice models. The predicted meltwater loading terms ΔZ_2 are, however, variable from site to site with maximum values ranging from less than 1 m at Cape York to more than 4 m at Port Pirie. In particular, these terms are quite different for sites within gulfs, such as at Port Pirie and Cape Spencer, that are less than 300 km apart along the margin of Spencer Gulf, and for the Queensland sites at Cape York, Halifax Bay and Karumba. These local and regional variations arise from the geometry of the shoreline in the vicinity of the point at which the RSL is evaluated; at Port Pirie and Karumba the sector of the crust subjected to water loading is restricted to relatively narrow azimuth ranges whereas at Cape Spencer or Cape York the crust is loaded over much larger azimuth ranges.

Figure 7(b) shows the same functions for the Pacific

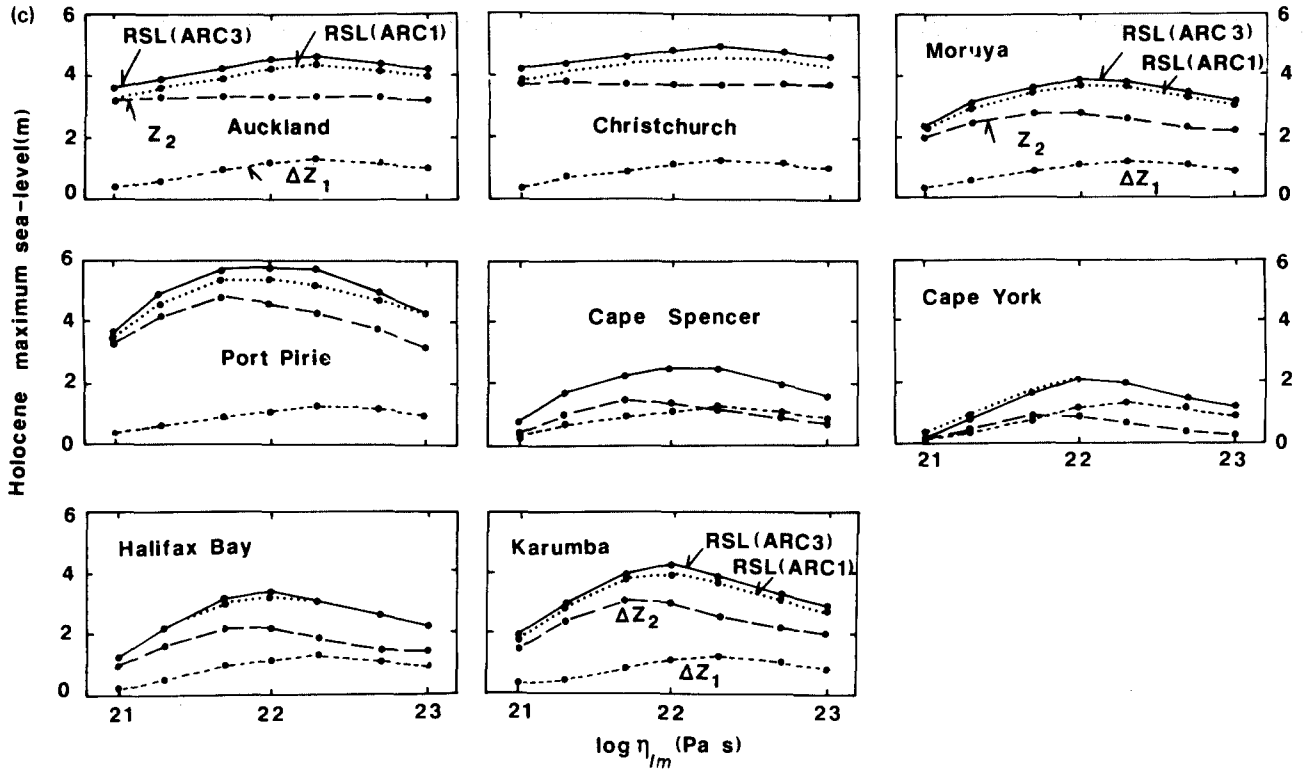

Figure 7. (c)—see caption opposite.

islands. Here the ice unloading terms ΔZ_1 for Fiji, Tahiti, Vahitahi (in the Tuamoto group) and Rarotonga are very similar but they differ from those predicted for Oahu, Hawaii, which lies closer to the former ice load. The meltwater loading terms ΔZ_2 are relatively insensitive to the lower mantle viscosity for all these islands but the amplitudes vary according to the size of the island; the larger the surface area, the larger ΔZ_2 (see also Nakada 1986). Fig. 7(c) illustrates results similar to Fig. 7(a) but, in this case, for the Antarctic ice load ANT 3. The characteristics of the meltwater loading term ΔZ_2 is generally the same as for the Arctic ice loads although the amplitudes are much reduced. The Antarctic ice unloading term ΔZ_1 does exhibit a different dependence on the lower mantle viscosity than does the corresponding Arctic term. Compare, for example, the sites closest to Antarctica, Christchurch, with sites much further from the load, such as Karumba.

In the above analyses the lithospheric thickness H has been assumed to be 50 km but the above results remain valid for $50 \lesssim H \lesssim 100$ km. It has been argued by Peltier (1984) that the lithospheric thickness, as estimated from glacial rebound data along the Atlantic margin of North America, is of the order of 200 km but Nakada & Lambeck (1988a) have shown that this is a consequence of inadequate spatial and temporal resolution of his adopted ice model. It may also be argued whether or not this parameter can be separated from the upper mantle viscosity, particularly from the far-field data alone. Fig. 8(a) illustrates the Holocene high-stand for a 50 km thick lithosphere and a 10^{21} Pa s^{-1} lower mantle viscosity as a function of upper mantle viscosity. The predicted high-stands at Karumba, Halifax Bay, Cape Spencer and Rarotonga are not strongly dependent on the upper mantle viscosity within the relatively restricted range of 10^{20}–10^{21} Pa s^{-1} but the high-stands for Port Pirie, Fiji and Christchurch are variable over this viscosity range. Fig. 8(b) illustrates the Holocene high-stands for a uniform mantle viscosity of 10^{21} Pa s^{-1} and for a variable lithospheric thickness H in the range of 50–220 km. Here the sites that are sensitive to lithospheric thickness (e.g. Fiji) are also sensitive to upper mantle viscosity and sites that are insensitive to H are also insensitive to η_{um} and for these continental margin and island sites it will not be possible to separate with confidence the parameters H and η_{um}. At sites such as Christchurch a 50 km thick lithosphere with an upper mantle viscosity of 2×10^{20} Pa s^{-1} gives about the same Holocene high-stand amplitude as a lithosphere of 220 km thickness overlying a 10^{21} Pa s^{-1} viscosity upper mantle. Because of this interdependence of H and η_{um} it is not possible to examine from this data alone whether the oceanic upper mantle has a low viscosity channel immediately below the lithosphere. For the present purpose a lithospheric thickness of 50 km has been adopted throughout although it is important to establish better bounds on this parameter. None of the following results for continental margin sites is significantly modified if this thickness is increased to 80 or even 100 km.

Figure 9 illustrates the dependence of the amplitude of the Holocene high-stand on both upper (η_{um}) and lower (η_{lm}) mantle viscosity in the respective ranges of 5×10^{19}–10^{21} and 10^{21}–10^{23} Pa s^{-1} for a 50 km thick lithosphere and the ice load ARC 3 + ANT 3. At sites such as Auckland and Christchurch the Earth's response is predominantly a function of the upper mantle viscosity,

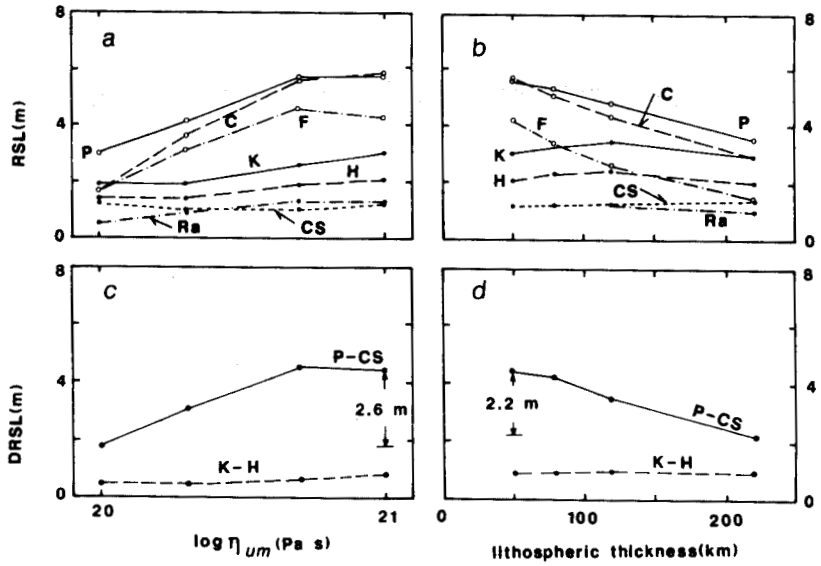

Figure 8. (a) Relative sea-levels (RSL) as a function of upper mantle viscosity for a lower mantle viscosity of 10^{21} Pa s^{-1} and a lithospheric thickness of 50 km. (b) RSL as a function of lithospheric thickness for a uniform mantle viscosity of 10^{21} Pa s^{-1}. (c) Differential relative sea-levels (DRSL) as defined by equation (5), as a function of upper mantle viscosity, and (d) as a function of lithospheric thickness. C = Christchurch, CS = Cape Spencer, F = Fiji, H = Halifax Bay, K = Karumba, P = Port Pirie, Ra = Rarotonga.

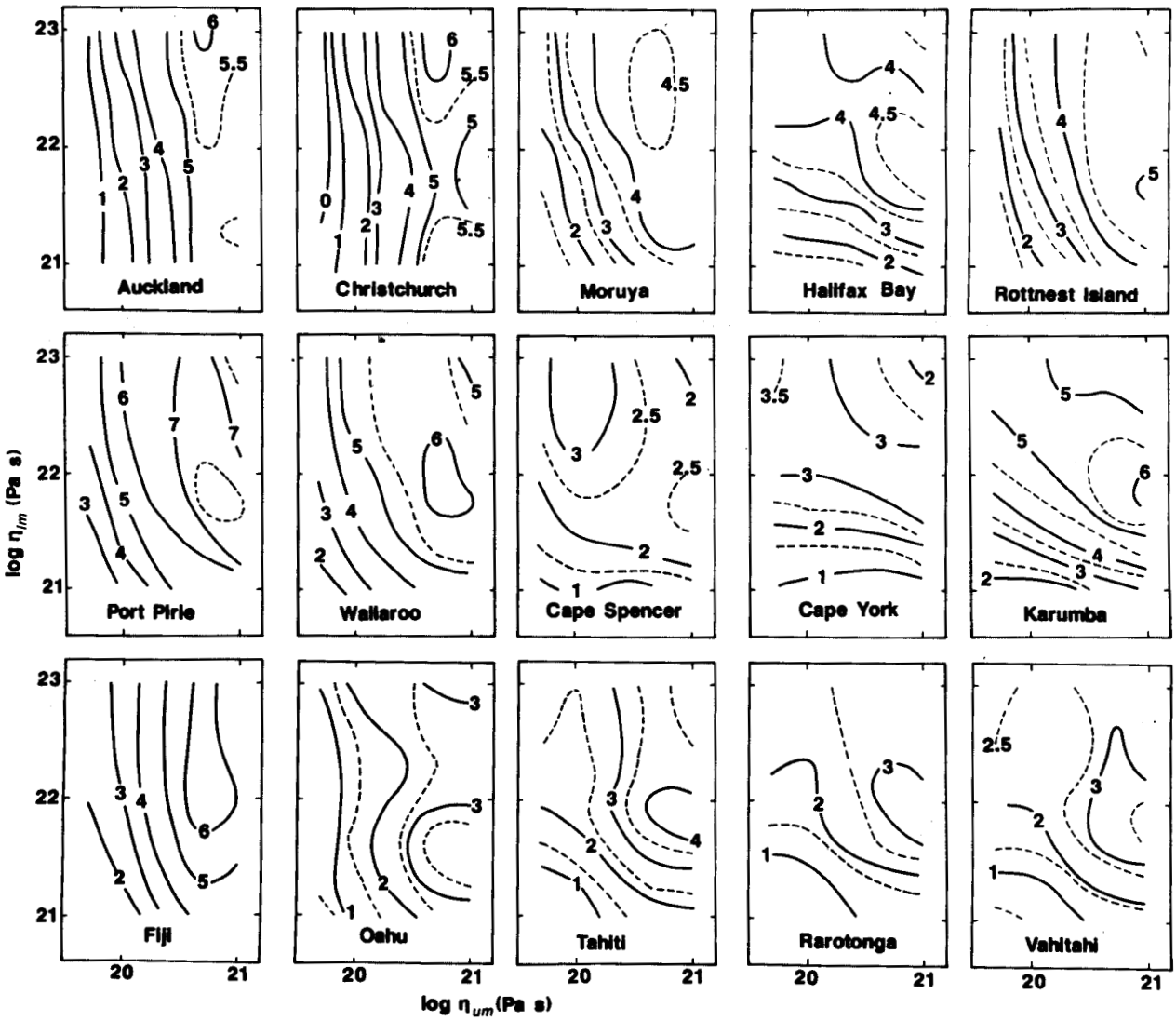

Figure 9. Predicted amplitudes of Holocene high-stands as a function of upper mantle η_{um} and lower mantle η_{lm} viscosities for selected continental margin and island sites with $H = 50$ km.

while at sites such as Cape York or Karumba the response is primarily controlled by the lower mantle viscosity and from observations at such sites it becomes possible to separate upper and lower mantle viscosities. Generally, the comparison of observations with these predictions suggests that $\eta_{um} \lesssim 10^{20}$ Pa s^{-1} and $\eta_{lm} \lesssim 10^{21}$ Pa s^{-1} for otherwise the predicted Holocene high-stands become much greater than the observed values.

Mantle models with these viscosity values, however, are unsatisfactory in several respects. First, the observed differential values of Late Holocene maxima are not well matched by these models for sites such as Karumba and Halifax where these sea-stands are well determined, or along the Spencer Gulf where large variations in the magnitude of the high-stand have been noted (Fig. 10).

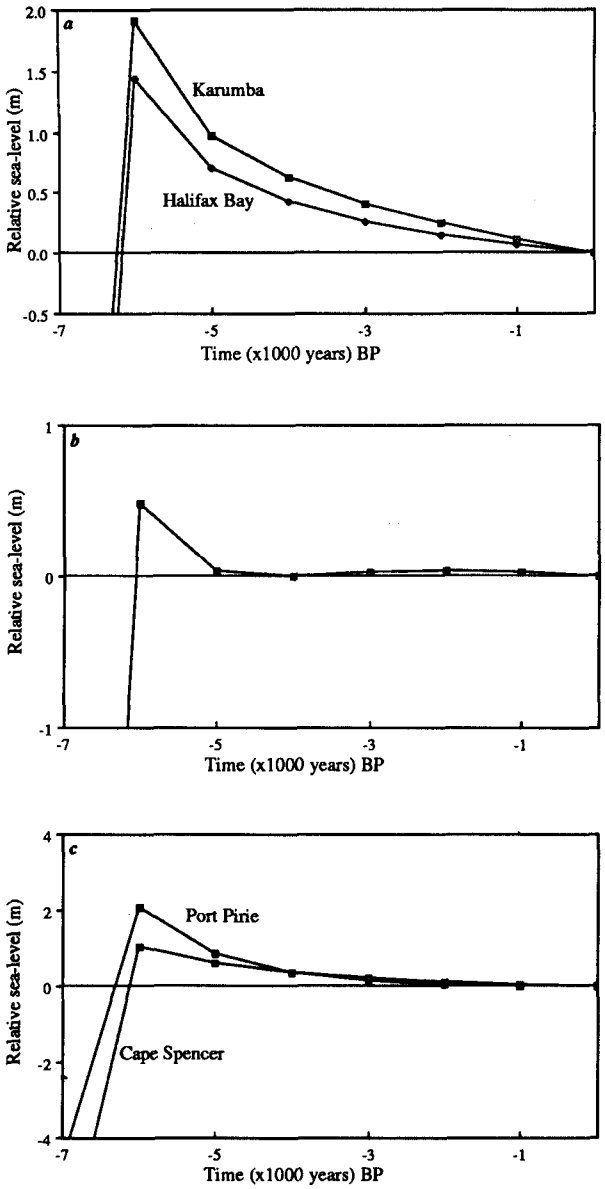

Figure 10. Relative sea-levels for Late Holocene time for $H = 50$ km, $\eta_{um} = 5 \times 10^{19}$ Pa s^{-1}, $\eta_{lm} = 10^{21}$ Pa s^{-1}. (a) For two sites in northern Queensland, Australia; (b) for a small island in French Polynesia; and (c) for two sites in Spencer Gulf, South Australia (cf. Figs 1 and 2).

Second, the models predict sea-level curves at small island sites, such as the Society and Tuamotu Islands, that are characterized by short-duration high-stands at about 6000 yr BP, in contrast with the observed values (Pirazzoli *et al.* 1987) (compare Figs 2 and 10). Third, for continental margin sites, the sea-levels are predicted to drop rapidly between about 6000 and 4000 yr BP and this is generally not observed (e.g. Chappell *et al.* 1983; Chappell 1987). For these reasons it is useful to explore the range of permissible mantle models more fully, using observations of the differences in sea-level from sites in the same general region.

DIFFERENTIAL HOLOCENE HIGH-STANDS

The above-discussed characteristics of the Holocene high-stands suggests that useful observational constraints are the differential sea-levels at locations in the same general region. The observed late Holocene high-stand ($\Delta\zeta_i^\circ$) at a tectonically stable site i can be written as (*cf.* equation 2)

$$\Delta\zeta_i^\circ = \Delta\zeta_{R,i} + \Delta Z_{1,i} + \Delta Z_{2,i}. \quad (4)$$

For the ice models ARC 1 to ARC 3 and ANT 1 to ANT 3, $\Delta\zeta_{R,i} = 0$ for $t < 6000$ yr but the following discussion is also valid when $\Delta\zeta_{R,i} \neq 0$ because this term is nearly constant for the far-field sites discussed here. The differential high-stand $d\zeta_{i,j}^\circ$ between sites i and j is then defined by

$$d\zeta_{i,j}^\circ = \Delta z_j^\circ - \Delta\zeta_i^\circ \simeq (\Delta Z_{1,j} - \Delta Z_{1,i}) + (\Delta Z_{2,j} - \Delta Z_{2,i}) \quad (5)$$

and is a function of the Earth's viscosity structure and of the rates of melting during the time interval from 18 000 to 6000 yr BP. The sea-levels prior to 6000 yr BP have previously been used to place gross constraints on the ice volumes and on the rates of melting of the Antarctic ice sheet and, within the range of melt models considered here, the differential sea-levels (5) are primarily sensitive to the rheological structure (Nakada & Lambeck 1988b). They do not, however, contribute greatly to separating the lithospheric thickness from upper mantle viscosity estimates (Figs 8c, d).

Differential Holocene sea-level maxima, as defined by eqn (5), are illustrated in Fig. 11(a) for selected pairs of sites and as a function of upper and lower mantle viscosities. For the sites at Karumba and Halifax Bay in northern Queensland, the observed differential high-stand is $\gtrsim 1.0$ m and this defines a broad range of upper and lower mantle viscosities that yield predictions that are consistent with the observations. For the sites Halifax Bay and Moruya along the eastern margin of Australia the observed differential high-stand lies between 0.0 and 1.5 m and this defines a further range of permissible effective viscosities for the two parts of the mantle. Likewise, the differential Holocene high-stand for the two nearby sites of Port Pirie and Cape Spencer in South Australia provides a further constraint and the three sets of differential values along the Australian margin define a relatively restricted range of values in η_{lm}–η_{um} space that are consistent with the observations; of $10^{20} \lesssim \eta_{um} \lesssim 2 \times 10^{20}$ Pa s^{-1} and $\eta_{lm} \gtrsim 5 \times 10^{21}$ Pa s^{-1} (Fig. 11a). If Christchurch is considered to be representative of a continental margin site then the differential heights between Moruya and Christchurch places a considerably tighter constraint on both the average upper and lower mantle viscosities as ($10^{20} < \eta_{um} < 2 \times 10^{20}$) Pa s^{-1} and ($5 \times 10^{21} <$

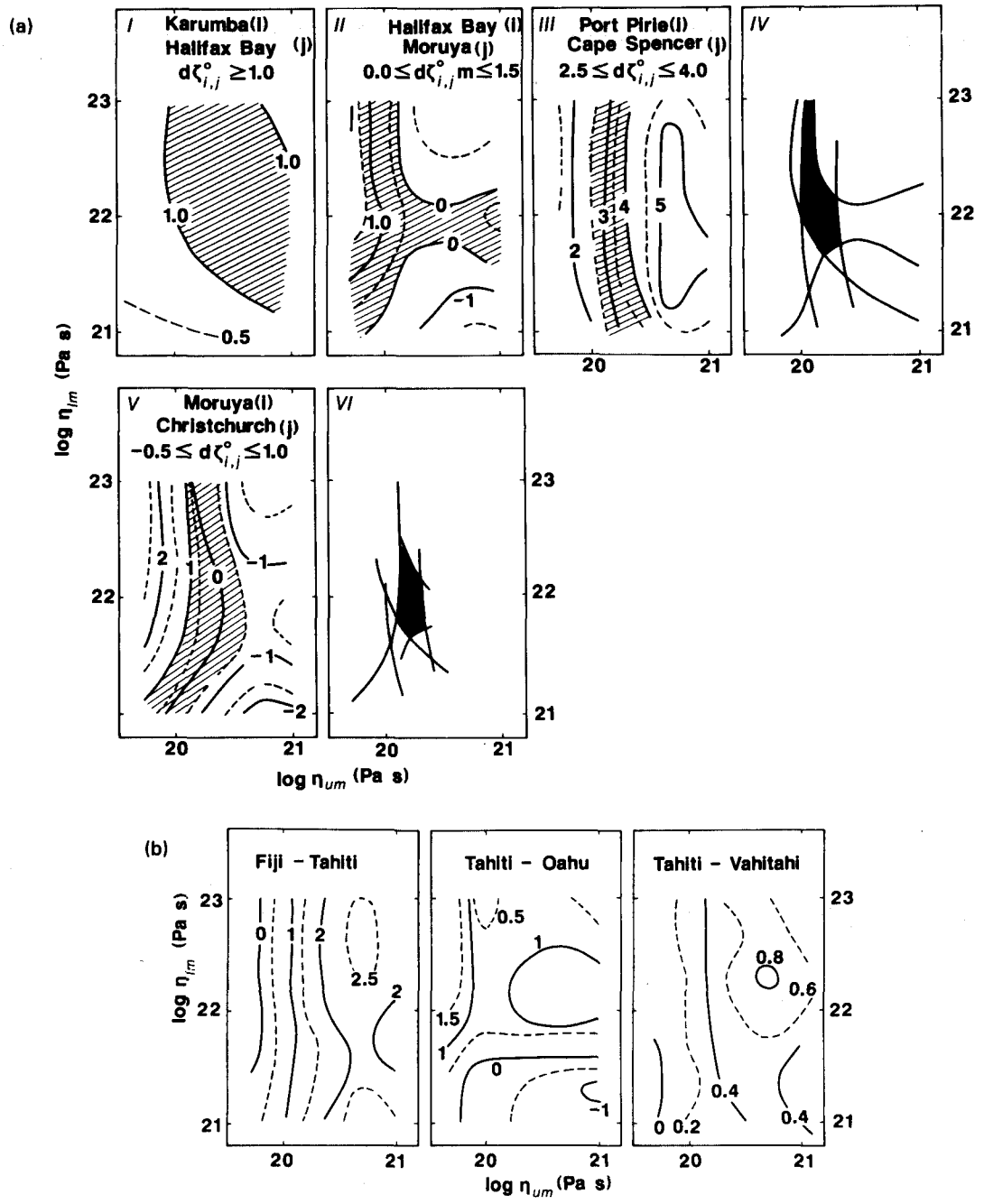

Figure 11. Predicted differential sea-levels as a function of upper and lower mantle viscosities and for $H = 50$ km. The shaded regions for each pair of sites indicates the range of permissible viscosity solutions. (a) For continental margin sites where (iv) illustrates that part of the viscosity range satisfied by the individual solutions (i)–(iii), and (vi) illustrates the solution if Christchurch is included as a continental margin site. (b) For some Pacific island sites.

$\eta_{lm} < 3 \times 10^{22}$) Pa s^{-1} respectively (Fig. 11a). To further constrain this solution for effective viscosity, particularly to place an upper bound on the lower mantle viscosity, requires further observations from pairs of sites whose differential response is particularly sensitive to the lower mantle structure. Differential sea-levels between the nearby islands of Tahiti and Vahitahi illustrate the effect of island size (Fig. 11b). According to Pirazzoli *et al.* (1987) the Holocene high-stand at Vahitahi was about 0.7 m, similar to that for Tahiti (Pirazzoli *et al.* 1985), and the small differential value supports an upper mantle viscosity of $\lesssim 10^{20}$ Pa s^{-1}. The difference Fiji–Tahiti, is likewise quite sensitive to upper mantle viscosity. The Holocene high-stand for Fiji has been estimated at up to 1.6 m above the present level (Hopley 1987) and the differential value with Tahiti also indicates that $\eta_{um} \lesssim 10^{20}$ Pa s^{-1}. Both the Fiji and Tahiti observations, however, are not very reliable and the islands may be subject to vertical movements as well, and while this suggestion is tempting, it is premature to conclude that upper mantle viscosity beneath the oceans is less than that beneath the continental margins. Differential sea-levels between Tahiti and Oahu, islands of about equal

size, are also illustrated in Fig. 11(b) and these are indicative of a particular sensitivity to the lower mantle rheology. Again the question of island stability needs to be examined before conclusions can be drawn about mantle rheology but these examples illustrate clearly the importance of island data for establishing whether lateral variations occur in mantle rheology.

AN ADJUSTMENT OF THE MELTING MODELS

With the solution $\eta_{um} \sim (1\text{–}2) \times 10^{20}$ Pa s^{-1} and $\eta_{lm} \simeq 10^{22}$ Pa s^{-1} that satisfies the differential sea-levels and with the ice models ARC 3 + ANT 3, the predicted absolute Holocene high-stand values are significantly greater than the observed values (Fig. 11a). Increasing the volume of meltwater that has been added into the oceans prior to about 8000 yr BP only increases this discrepancy while a decrease in the Antarctic contributions does not modify the result greatly either. Fig. 12(b), for example, illustrates the result for an Antarctic model (ANT 4) in which the total meltwater volume has been reduced to an equivalent sea-level rise of 23 m and in which melting did not start until about 12 000 yr BP (see also Fig. 3).

Recourse to the argument of tectonic instability of the sites is not satisfactory in that it requires that all sites used here have subsided at rates of the order of about 0.2–0.4 mm yr^{-1} but there is no independent geological evidence to support such an interpretation; in particular, if this were so the inter-glacial maximum high-stand at 120 000 yr BP would now be between 20 and 40 m below present sea-levels whereas it is usually observed to lie at a few metres above the present level (e.g. Chappell 1987). An alternate explanation is to assume that minor deglaciation continued throughout late-Holocene time. The Laurentide ice sheet disappeared completely by about 6000 yr BP (e.g. Prest 1969) while the Fennoscandian ice sheet vanished at a much earlier date (de Geer 1954), but there is no evidence that the deglaciation of the Antarctic ice sheet also ceased at 6000 yr BP (Denton & Hughes 1981; Pickard 1986). In particular, if this latter deglaciation is controlled by the rising sea-level, then minor melting may have continued well into mid- to late-Holocene time. Fig. 13 illustrates the equivalent sea-level curve for the past 8000 yr based on the model ANT 3. This model can be adjusted such that the predicted differential Holocene high-stand values are preserved and the absolute values are consistent with the observational evidence. The amount by which the ice model is adjusted is now a function of the mantle parameters although, within the range of mantle parameters that produce satisfactory differential Holocene levels, this dependence is slight. Fig. 13 illustrates two models ANT 3A and ANT 3B which are based on a lower mantle viscosity of 10^{22} Pa s^{-1}, a lithospheric thickness of 50 km, and upper mantle viscosities of 10^{20} and 2×10^{20} Pa s^{-1}, respectively (Nakada & Lambeck 1988b). Both produce very similar

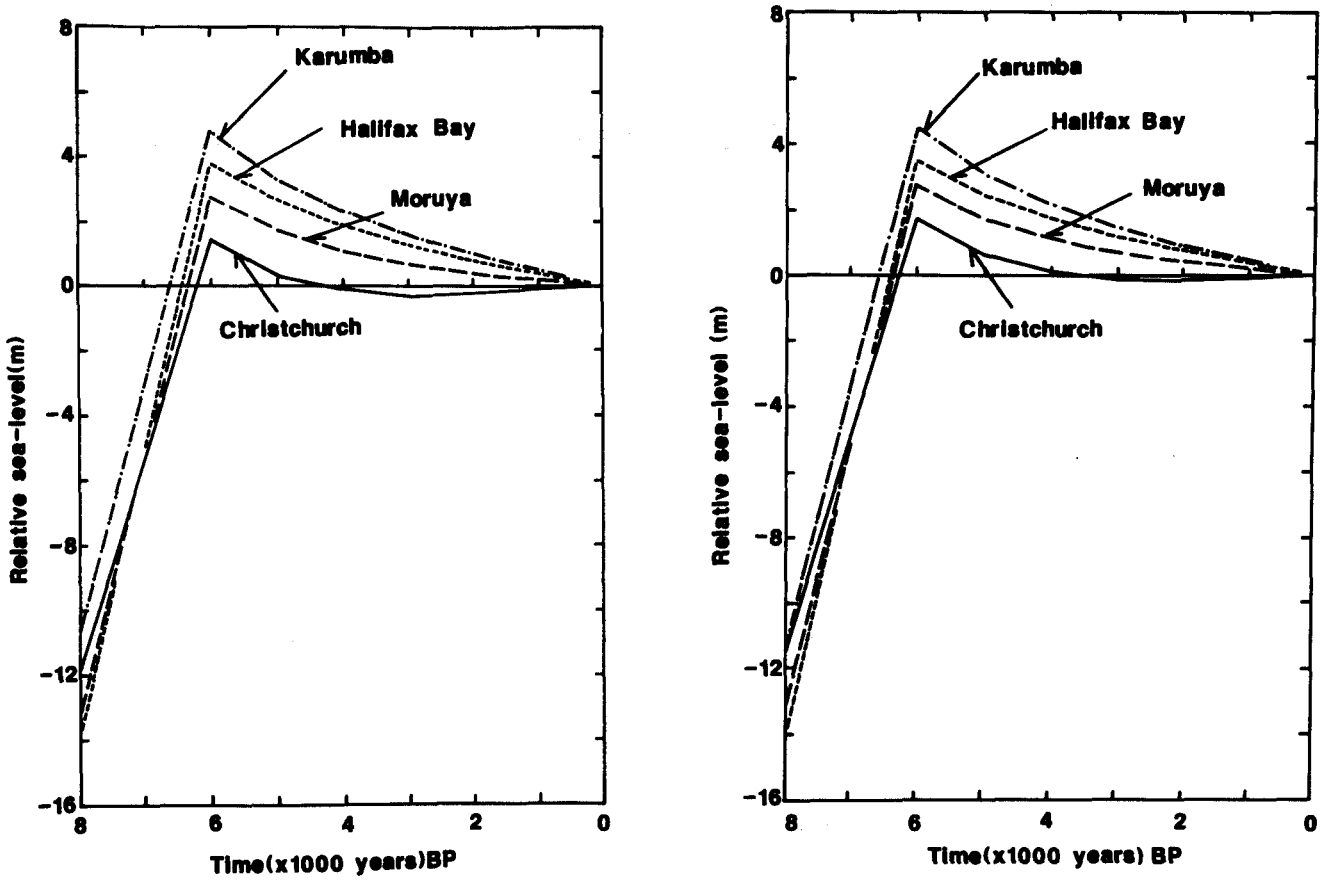

Figure 12. Predicted Holocene sea-levels for continental margin sites for the ice models (a) ARC 3 + NT 3 and (b) ARC 3 + ANT 4 (see Fig. 3), and lithospheric thickness, upper mantle viscosity and lower mantle viscosity of 50 km, 10^{20} and 10^{22} Pa s^{-1}, respectively.

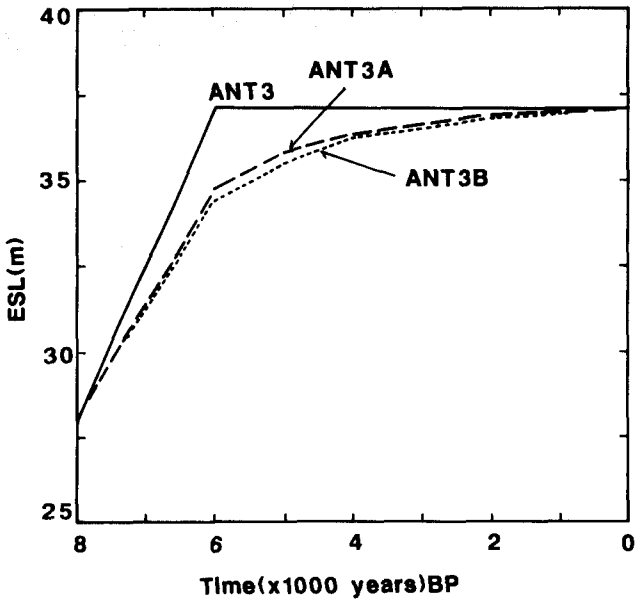

Figure 13. Equivalent sea-levels for the Antarctic ice models ANT 3, ANT 3A and ANT 3B based on Holocene sea-level observations.

results for the Holocene sea-levels as is illustrated in Fig. 14 and now the predicted Holocene high-stands agree well with the observed values at most of the sites examined. At Port Pirie, for example, the maximum amplitude is about 3 m while the Cape Spencer sea-levels did not rise significantly above the present level; the New Zealand sea-levels are predicted to have had zero or very small Holocene high-stands and the Pacific island high-stands are also much reduced and, particularly for small islands, these high-stands now occur later, between about 4000 and 2000 yr ago.

DISCUSSION

Holocene high-stands along continental margins

Fig. 15 illustrates the predicted regional variability in the sea-level response in the Australian region for the following combination of ice and mantle models: (i) ARC 3 + ANT 3A, $H = 50$ km, $\eta_{um} = 10^{20}$ Pa s^{-1}, $\eta_{lm} = 10^{22}$ Pa s^{-1}, and (ii) ARC 3 + ANT 3B, $H = 50$ km, $\eta_{um} = 2 \times 10^{20}$ Pa s^{-1}, $\eta_{lm} = 10^{22}$ Pa s^{-1}. As previously noted, values of H of up to 100 km produce similar results. One feature of these solutions is the general increase in the amplitudes of the Holocene high-stands with decreasing latitude or with increasing distance from Antarctica, in agreement with the general trend observed from south to north along the eastern margin of Australia (cf. Fig. 1). In particular, no Holocene high-stand is predicted for Tasmania. This is a result of the Antarctic ice unloading term ΔZ_1 because no modification of the Arctic ice sheets can produce such a regional trend, and it supports the argument that Antarctic melting in Late Pleistocene time was significant and that this melting occurred at approximately the same time as the Arctic melting. A second feature of these solutions is the

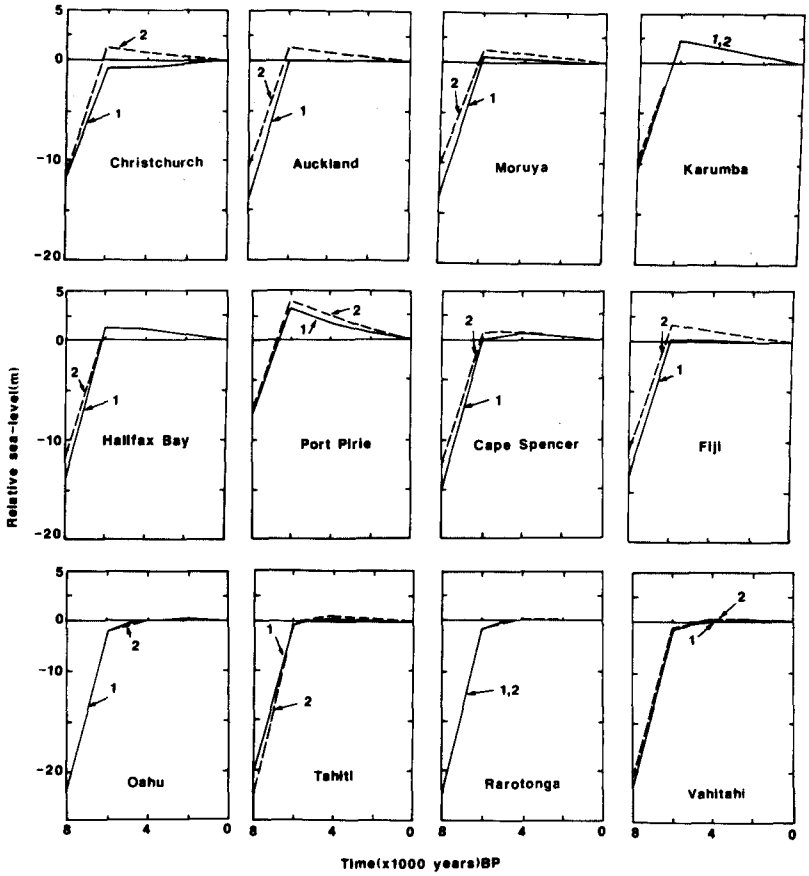

Figure 14. Relative sea-levels corresponding to the models with $H = 50$ km, $\eta_{lm} = 10^{22}$ Pa s^{-1} and (1) ARC 3 + ANT 3A, for $\eta_{um} = 10^{20}$ Pa s^{-1}, and (2) ARC 3 + ANT 3B for $\eta_{um} = 2 \times 10^{20}$ Pa s^{-1}.

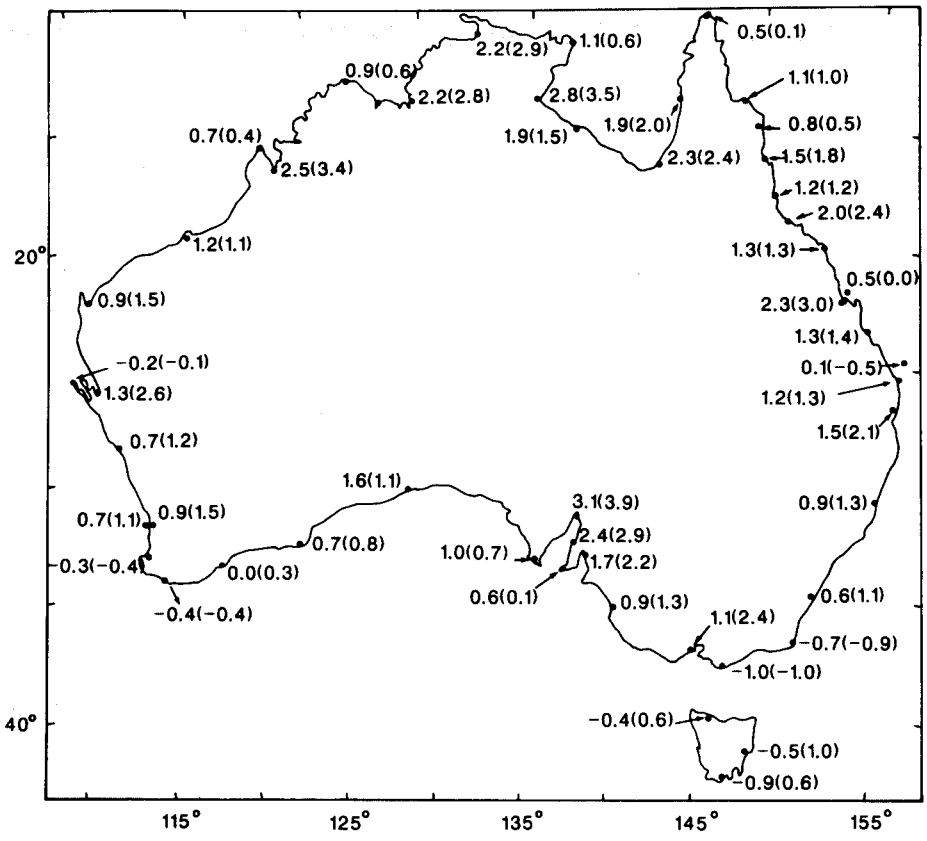

Figure 15. Predicted Holocene sea-levels at 6000 yr BP along the Australian margin for two ice–mantle models. The first number corresponds to the combination ARC 3 + ANT 3A and an upper mantle viscosity of 10^{20} Pa s^{-1}. The second number, in parenthesis, corresponds to ARC 3 + ANT 3B and an upper mantle viscosity of 2×10^{20} Pa s^{-1}. In both, the lower mantle viscosity is 10^{22} Pa s^{-1} and the lithospheric thickness is 50 km.

shorter wavelength variability in the sea-level response as a consequence of the coastline geometry such as is predicted to occur in the Spencer Gulf and the Gulf of Carpentaria, where the high-stands are larger at sites within the gulfs than at sites on neighbouring peninsulas. Even for relatively small coastal identations, such as occur along the Queensland coast, significant regional variation is predicted and the examination of sea-level indicators at such sites is particularly important for studies of the lithospheric and upper mantle response to surface loading.

Tilting of continental margins and timing of high-stands

Another feature of the models is that they predict significant tilting of the continental shelves, the Holocene high-stands, for example, decreasing in amplitude with distance outwards from the present shoreline: predicted high-stands for the outer part of the Great Barrier Reef are small or zero in amplitude and occur much later in time than at sites on the inner reefs or on the coast (Fig. 16). There is indeed observational evidence for this. For example, Chappell *et al.* (1983) study of the age–height distribution of micro-atolls from North Queensland point to higher Holocene sea-levels from samples on the mainland coast at Yule Point than from the samples from reefs on the inner shelf, possibly by as much as 0.7 m. Also, while a Holocene high-stand has developed along the mainland Queensland coast and at near-offshore islands and reefs, it is absent at outer reef locations (see also Hopley 1983b). A potentially important observation is that the tilting of the continental shelf is quite sensitive to the upper mantle viscosity, as is illustrated in Fig. 17.

Rigorous modelling of this tilting of the margin requires consideration of the migration of the shoreline with time as sea-levels rises, an effect that may be particularly important in shallow sea areas, such as the Gulf of Carpentaria, where average present water depths are less than about 100 m. Approximate models of rebound with time-dependent ocean functions indicate that this effect on the relative sea-level curve may be of the order of 10 per cent for sites such as Karumba and along the Queensland coast.

A consequence of the tilting of the shelf is that it produces a regional variation of the time at which the Holocene high-stand maxima first occurred or of the time at which sea-level first reached its present value, if this level was reached at all. Along the continental margins these levels are predicted to have been reached at about 6500–6000 yr BP, with the earliest ages occurring at the southernmost sites. At island sites, however, these levels are predicted to occur by as much as 2000 yr later. This is also in general agreement with observations along the north Queensland coast. For example, on the islands of Orpheus and Rattlesnake which lie about 10–15 km from the mainland, the present sea-level was reached about

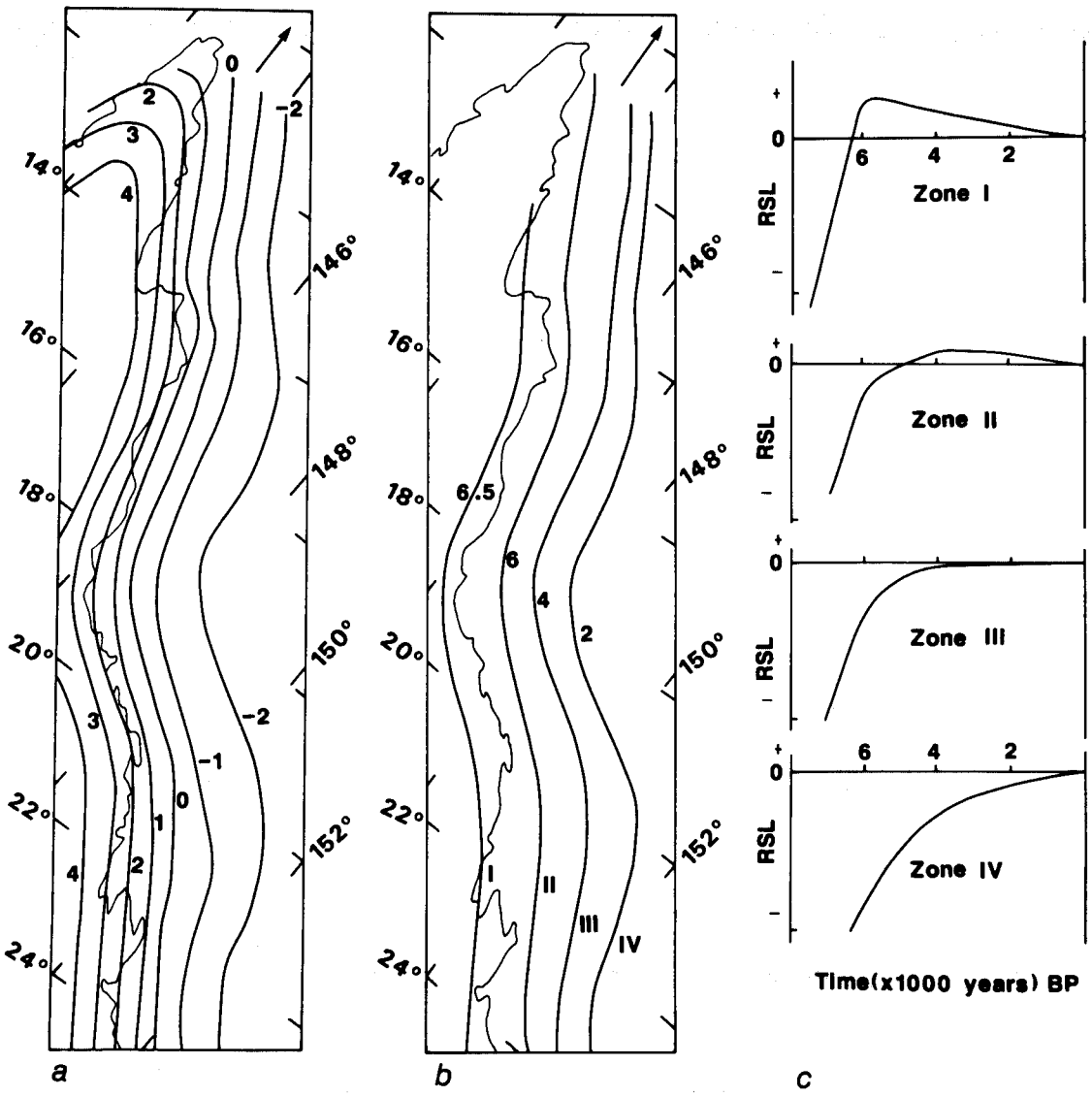

Figure 16. (a) Predicted Holocene sea-levels (in metres) at 6000 yr BP, and (b) the times at which sea-level first reached its present value (in 1000 yr) along the margin and Great Barrier Reef of northern Queensland for the model ARC 3 + ANT 3B, $\eta_{um} = 2 \times 10^{20}$ Pa s^{-1}, $H = 50$ km and $\eta_{lm} = 10^{22}$ Pa s^{-1}. The characteristic sea-level curves in the four zones indicated in (b) are illustrated in (c).

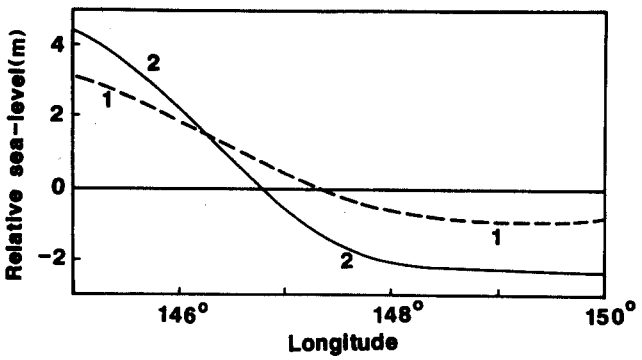

Figure 17. Tilting of the continental edge along 18 °S across the north Queensland coast for two models (1) ARC 3 + ANT 3A and $\eta_{um} = 10^{20}$ Pa s^{-1}, and (2) ARC 3 + ANT 3B and $\eta_{um} = 2 \times 10^{20}$ Pa s^{-1}.

5500–6000 yr BP but at Grub and Wheeler Reefs, which lie about 80 km from the mainland, sea-levels did not approach their present levels until about 2000 yr later (Hopley 1983a). The sea-level indicators in these examples are based on reef cores and they assume that reef growth kept up with the rising water level and the actual levels would lie above these data, but the significant observation is the difference between the two regions, a difference that is generally consistent with the predictions illustrated in Fig. 16. This difference has usually been attributed to reef accretion lagging behind sea-level change by amounts that vary with distance from the continental margin (e.g. Hopley 1983; Davies & Hopley 1983a) but these model calculations illustrate that it may, at least in part, also reflect the differential sea-level change in the region, with quite significant variations in response occurring across the shelf over distances of the order of 100 km.

The predicted regional variability of the Holocene high-stand for northern Queensland is similar to that

predicted by Chappell *et al.* (1982) who computed the deformation produced by the water loading only, equivalent to the ΔZ_2 term, using a one-dimensional model along several sections across the continental margin. This latter calculation does not impose the condition that water surfaces must be equipotential surfaces at all times but this effect will be small in the Late Holocene far-field and all meltwater has been added into the oceans. The good agreement between the two approaches suggests that for these far-field sites it may be appropriate and convenient to compute the Late Holocene sea-level changes in two parts in which the global spherical model is used to establish the regional contribution arising from the ice unloading effect and a more local and flat earth model is used to compute the contributions resulting from the deformation of the crust in response to the change in water load in the vicinity of the site. This approach may be particularly useful for areas where complex coastal geometry is not readily resolved with the global models used here, as along, for example, the upper reaches of Spencer Gulf.

Holocene sea-levels in the SW Pacific

Some characteristic sea-level responses predicted for island sites in the SW Pacific are illustrated in Fig. 14. Throughout this region the ice-unloading term ΔZ_1 is quite constant although it does change for sites further to the north such as Oahu. Differential sea-levels between Oahu and Tahiti, for example, would be quite sensitive indicators of lower-mantle viscosity if tectonic subsidence of both islands could be excluded (Fig. 11b). The amplitude of the meltwater term, ΔZ_2, throughout the region is insensitive to the value of the lower mantle viscosity but it is a function of the island size, and differential sea-levels between small and large islands in the same region (e.g. Fiji and Tahiti and to a lesser degree Tahiti and Vahitahi) are predominantly sensitive to the upper mantle viscosity (Fig. 11b). Simple regional patterns for the sea-level change in the world's oceans do not, therefore, exist. Important for geophysics is that indicators of sea-level change from sites selected because of their particular sensitivity to mantle rheology parameters, provide important information on mantle rheology, always assuming that the sites themselves are not subject to tectonic movements as may be the case for islands near plate margins or for young volcanic islands. This warrants further examination.

At many of the Pacific sites the time at which sea-level last reached its present value is more recent than for continental margin sites and the maximum late Holocene sea-level often occurs in the interval 4000–2000 yr BP (see, for example, fig. 13.9 of Hopley 1987). Predictions based on ice models in which all melting ceased at 6000 yr BP invariably produce high-stands at about this time whereas models in which some Antarctic melting is permitted in Late Holocene time predict Holocene sea-level maxima that are smaller in amplitude, which occur later by about 2000 yr and which remain near their maximum level for about 1000–2000 yr (Fig. 18), in general agreement with observations.

Antarctic melting

The conclusion that a small amount of meltwater (equivalent to a total of about 10^6 km^3 of grounded ice

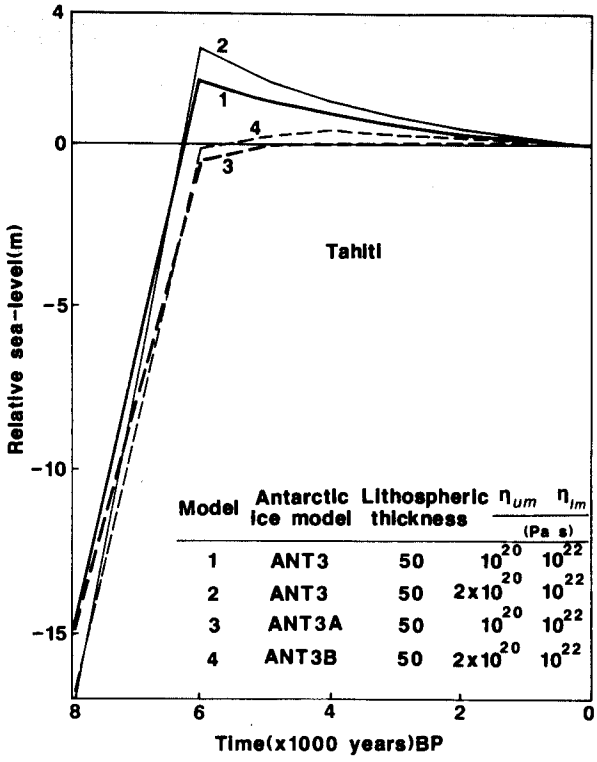

Model	Antarctic ice model	Lithospheric thickness	η_{um} (Pa s)	η_{lm} (Pa s)
1	ANT3	50	10^{20}	10^{22}
2	ANT3	50	2×10^{20}	10^{22}
3	ANT3A	50	10^{20}	10^{22}
4	ANT3B	50	2×10^{20}	10^{22}

Figure 18. Predicted Holocene sea-levels for Tahiti for four different models. Observations indicate a maximum level of about 0.5 m occurring at about 3000 yr BP, consistent with model 4 (ARC 3 + ANT 3B, $\eta_{um} = 2 \times 10^{20}$ Pa s^{-1}).

above sea-level) continued to be added into the oceans between 6000 yr BP and the present is consistent with observations of ice retreat in the Vestfold Hills of Antarctica up to the present (Adamson & Pickard 1986). To effect a change in global sea-level of 1 m from Antarctic land ice, an average retreat by about 10 km of the Antarctic ice margin is required (Walcott 1974). Much of this margin is difficult to examine but according to Adamson & Pickard, the rate of ice retreat in the Vestfold Hills during late Holocene time has averaged about 2–3 m yr^{-1}, while Stuiver *et al.* (1981) have concluded that a slow Late Holocene retreat of the ice margins in the Ross and Weddell Seas cannot be excluded from the available data.

The conclusion concerning ongoing Antarctic melting into Late Holocene time is consistent with our earlier suggestion that the far-field sea-level observations in the time interval of 10 000–6000 yr BP are indicative of Antarctic melting having occurred somewhat later than the Arctic melting and lends support to the models in which the decay of the Antarctic ice sheet is triggered in whole or in part by the rise in sea-level produced by the earlier melting of the Arctic ice sheet (e.g. Stuiver *et al.* 1981; Budd & Smith 1982). With the present sea-level data it is not possible to identify which part of the Antarctic contributes most to this late Pleistocene and early Holocene meltwater and what is needed to do this are sea-levels closer to Antarctica, or from the Antarctic margin itself.

Tectonic movements

The regional variations in sea-level resulting from the effect of meltwater loading can be sufficiently large in some

instances to be confused with tectonic movements. It has, for example, been proposed by Belperio *et al.* (1984) that the Spencer Gulf data is indicative of differential tectonic movements but clearly this conclusion is not warranted as much of the regional variability can be explained in terms of the meltwater loading. Similarly, it has been suggested that some of the regional sea-level variations along the North Queensland coast are indicative of tectonic movement although Hopley (1983b) recognized that this could also be a consequence of the Earth's response to water loading. A third area where regional tectonics has been suggested is near Perth, Western Australia, where the model predictions for the area range between about 0.7 and 1.5 m (Fig. 15). Holocene highs of about 3 m have been reported for Rottnest Island (Playford 1987) and about 2.5 m to the south of Perth (Searle & Woods 1986) whereas Kendrick (1977) reported only about 0.5 m in the Swan River Estuary near Perth. The region over which the observed variations occur is too small to be attributed to the variable response of the Earth to meltwater loading and if all observations are correct then there indeed has been differential tectonic uplift in the area (Lambeck 1987). A wide range of models for the Earth's response and for the ice loads has been examined but no model explains the observations of Holocene maxima of 2.5–3 m without destroying the general agreement at all other Australian sites. The lower value observed in the Swan River estuary is more consistent with the models. In view of the potential of this observation to constrain the mantle rheology models (Fig. 11b), these observations warrant closer examination.

A further possible discrepancy between the predictions of Fig. 15 and observations (Fig. 1) occurs along the NW margin of Australia. Holocene high-stands of about 1 m have been reported for the Fitzroy and Ord River estuaries (Brown 1983) and of less than 1 m for the Alligator River estuary (Woodroffe *et al.* 1987) compared with predicted values of 2–3 m for these estuaries. Neither has evidence been found in this region for the last interglacial high-stand which occurs elsewhere at a few metres above present sea-level. Unless lateral variations in viscosity or lithospheric thickness can explain these observations, one is forced to conclude that the NW region of Australia has been subjected to subsidence at a rate of about 1 m in 6000 yr (see also Woodroffe *et al.* 1987).

Mantle and lithospheric parameters

While the observations examined here are strongly suggestive of an increase in mantle viscosity with depth, they do not suffice to give a unique determination of the depth dependence of viscosity. In particular, it remains difficult to separate the effects of lithospheric thickness and upper mantle viscosity, particularly if low viscosity channels are introduced. The mantle models proposed here are therefore 'effective' models which, for the continental margin sites, can be characterized by an average lithospheric thickness of 50–100 km, an upper mantle viscosity of $(1–2)10^{20}$ Pa s^{-1} down to 670 km, and a lower mantle viscosity of about 10^{22} Pa s^{-1}. The ocean island data are suggestive of a somewhat lower value for the upper mantle viscosity but these observations are also questionable because of the possible occurrence of vertical movements, and they warrant further study. More important than these values themselves is the demonstration that by examining differential sea-levels in the far-field it becomes possible to separate the effective mantle response parameters from the uncertainties associated with the melting histories of the ice caps and that by using differential values between continental margins and mid-ocean island sites it becomes possible to examine whether lateral variations occur in these effective parameters.

ACKNOWLEDGMENTS

We thank Drs J. Chappell and D. Hopley for valuable discussions on the Australasian evidence for sea-level change.

REFERENCES

Adamson, D. A. & Pickard, J., 1986. Cainozoic history of the Vestfold Hills, in *Antarctic Oasis*, pp. 63–93, ed. Pickard, J., Academic Press, Sydney.

Belperio, A. P., Hails, J. R. & Gostin, V. A., 1983. A review of Holocene sea levels in South Australia, in *Australian Sea Levels in the Last 15000 Years: A Review*, Monograph Series, Occasional Paper, 3, pp. 37–47, ed. Hopley, D., Department of Geography, James Cook University of North Queensland.

Belperio, A. P., Hails, J. R., Gostin, V. A. & Polach, H. A., 1984. The stratigraphy of coastal carbonate banks and Holocene sea levels of northern Spencer Gulf, South Australia, *Mar. Geol.*, **61**, 297–313.

Bloom, A. L., 1967. Pleistocene shorelines: A new test of isostasy, *Bull. geol. Soc. Am.*, **78**, 1477–1494.

Brown, R. G., 1983. Sea-level history over the past 15,000 years along the Western Australian region, in *Australian Sea Levels in the Last 15000 Years: A Review*, Monograph Series, Occasional Paper, 3, pp. 29–36, ed. Hopley, D., Department of Geography, James Cook University of North Queensland.

Budd, W. F. & Smith, I. N., 1982. Large-scale numerical modelling of the Antarctic ice sheet, *Ann. Glaciol.*, **3**, 42–49.

Burne, R. V., 1982. Relative fall of Holocene sea level and coastal progradation, north eastern Spencer Gulf, South Australia, *BMR J. Aust. Geol. Geophys.*, **7**, 35–45.

Carter, R. M. & Johnson, D. P., 1986. Sea-level controls on the post-glacial development of the Great Barrier Reef, Queensland, *Mar. Geol.*, **71**, 137–164.

Cathles, L. M., 1975. *The Viscosity of the Earth's Mantle*, Princeton University Press, New Jersey.

Cathles, L. M., 1980. Interpretation of the postglacial isostatic adjustment phenomena in terms of mantle rheology, in *Earth Rheology, Isostasy and Eustasy*, ed. Mörner, N., Wiley, New York.

Chappell, J., 1974. Geology of coral terraces, Huon Peninsula, New Guinea: a study of Quaternary tectonic movements and sea-level changes, *Bull. geol. Soc. Am.*, **85**, 553–570.

Chappell, J., 1987. Late Quaternary sea-level changes in the Australian region, in *Sea-level Changes*, pp. 296–331, eds Tooley, M. J. & Shennan, I., Basil Blackwell, New York.

Chappell, J., Chivas, A., Wallensky, E., Polach, H. A. & Aharon, P., 1983. Holocene paleo-environmental changes, central to north Great Barrier Reef inner zone, *Bur. Min. Res. J. Aust. Geol. Geophys.*, **8**, 223–235.

Chappell, J., Rhodes, E. G., Thom, B. G. & Wallensky, E. P., 1982. Hydro-isostasy and the sea-level isobase of 5500 B.P. in north Queensland, Australia, *Mar. Geol.*, **49**, 81–90.

Chappell, J. & Shackleton, N. J., 1986. Oxygen isotopes and sea-level, *Nature*, **324**, 137–140.

Clark, J. A., Farrell, W. E. & Peltier, W. R., 1978. Global changes in postglacial sea level: a numerical calculation, *Quat. Res.*, **9**, 265–287.

Davies, P. J. & Hopley, D., 1983. Growth fabrics and growth rates of Holocene reefs in the Great Barrier Reef, *Bur. Min. Res. J. Aust. Geol. Geophys.*, **8**, 237–251.

De Geer, E. H., 1954. Skandinaviens geokronologi, *Geol. För. Stockh. Förh.*, **76,** 299–329.
Denton, G. H. & Hughes, T. J. (eds), 1981. *The Last Great Ice Sheets,* Wiley, New York.
Drewry, D. J. (ed.), 1982. *Antarctica: Glaciological and Geophysical Folio,* Scot Polar Res. Inst., Cambridge.
Dziewonski, A. M. & Anderson, D. L., 1981. Preliminary reference Earth model, *Phys. Earth planet. Int.*, **25,** 297–356.
Fairbridge, R. W., 1961. Eustatic changes in sea level, *Phys. Chem. Earth,* **4,** 99–184.
Farrell, W. E. & Clark, J. A., 1976. On postglacial sea-level, *Geophys. J. R. astr. Soc.*, **46,** 647–667.
Fjeldskaar, W. & Cathles, L. M., 1984. Measurement requirements for glacial uplift detection of nonadiabatic density gradients in the mantle, *J. geophys. Res.*, **89,** 10115–10124.
Gibb, J. G., 1986. A New Zealand regional Holocene eustatic sea-level curve and its application for determination of vertical tectonic movements, *Bull. R. Soc. New Zealand,* **24,** 377–395.
Hails, J. R., Belperio, A. P. & Gostin, V. A., 1984. Quaternary sea levels, northern Spencer Gulf, Australia, *Mar. Geol.*, **61,** 373–389.
Hopley, D., 1983a. Deformation of the north Queensland continental shelf in the Late Quaternary, in *Shorelines and Isostasy,* pp. 347–366, ed. Smith, D. E. & Dawson, A. G., Academic Press, London.
Hopley, D., 1983b. Evidence of 15,000 years of sea level change, in *Australian Sea Levels in the Last 15000 Years: A Review,* Monograph Series, Occasional Paper, 3, pp. 93–104, ed. Hopley, D., Department of Geography, James Cook University of North Queensland.
Hopley, D., 1987. Holocene sea-level changes in Australasia and southern Pacific, in *Sea Surface Studies: A Global Review,* pp. 375–408, ed. Devoy, R. J. N., Croom Helm, New York.
Hopley, D. & Thom, B. G., 1983 (eds). *Australian Sea Levels in the Last 15000 Years: A Review,* Monograph Series, Occasional Paper, 3, pp. 3–26. Department of Geography, James Cook University of North Queensland.
Jongsma, D., 1970. Eustatic sea-level changes in the Arafura Sea, *Nature,* **228,** 150–151.
Kaula, W. M., 1980. Problems in understanding vertical movements and Earth rheology, in *Earth Rheology, Isostasy and Eustasy,* pp. 577–588, ed. Mörner, A., Wiley, New York.
Kendrick, G. W., 1977. Middle Holocene marine molluscs from near Guildford, Western Australia, and evidence for climatic change, *J. R. Soc. West. Aust.*, **59,** 97–104.
Lambeck, K., 1987. The Perth Basin: a possible framework for its formation and evolution, *Explor. Geophys.*, **18,** 124–128.
Lambeck, K. & Nakada, M., 1985. Holocene fluctuations in sea-levels: constraint on mantle viscosity and melt-water sources, *Proc. Fifth Int. Coral Reef Congr., Tahiti,* **3,** 79–84.
Nakada, M., 1986. Holocene sea levels in oceanic islands: implications for the rheological structure of the Earth's mantle. *Tectonophys.*, **121,** 263–276.
Nakada, M. & Lambeck, K., 1987. Glacial rebound and relative sea-level variations: a new appraisal, *Geophys. J. R. astr. Soc.*, **90,** 171–224.
Nakada, M. & Lambeck, K., 1988a. Non-uniqueness of lithospheric thickness estimates based on glacial rebound data along the east coast of North America, in *Mathematical Geophysics,* pp. 347–361, eds Vlaar, N. J., Nolet, G., Wortel, M. J. R. & Cloetingh, S. A. P. L., Reidel, Dordrecht.
Nakada, M. & Lambeck, K., 1988b. The melting history of the late Pleistocene Antarctic ice sheet, *Nature,* **333,** 36–40, 1988.
Nakiboglu, S. M. & Lambeck, K., 1982. A study of the Earth's response to surface loading with application to Lake Bonneville, *Geophys. J.R. astr. Soc.*, **70,** 577–620.
Nakiboglu, S. M. & Lambeck, K., 1983. A re-evaluation of the isostatic rebound of Lake Bonneville, *J. geophys. Res.*, **88,** 10439–10447.
Nakiboglu, S. M., Lambeck, K. & Aharon, P., 1983. Postglacial sea-levels in the Pacific: implications with respect to deglaciation regime and local tectonics, *Tectonophys.*, **91,** 335–358.
Newman, W. S., Cinguomani, L. J., Pardi, R. R. & Marcus, L. F., 1980. Holocene delevelling of the United States' east coast, in *Earth Rheology, Isostasy and Eustasy,* ed. Mörner, N., Wiley, New York.
Ota, Y., Matsushima, Y. & Moriwaki, H., 1981. *Atlas of Holocene Sea Level Records in Japan,* Japanese working group of Holocene sea-level project, JGCP.
Passey, Q. R., 1981. Upper mantle viscosity derived from the differences in rebound of the Provo and Bonneville shorelines: Lake Bonneville Basin, Utah, *J. geophys. Res.*, **86,** 11701–11709.
Peltier, W. R., 1984. The thickness of the continental lithosphere, *J. geophys. Res.*, **89,** 11303–11316.
Peltier, W. R. Andrews, J. T., 1976. Glacial isostatic adjustment – I: The forward problem, *Geophys. J.R. astr. Soc.*, **46,** 605–646.
Pickard, J. (ed.), 1986. *Antarctic Oasis, Terrestrial Environments and History of the Vestfold Hills,* Academic Press, Sydney, Australia.
Pirazzoli, P. A. & Montaggioni, L. F., 1986. Late Holocene sea-level changes in the northwest Tuamotu Islands, French Polynesia, *Quat. Res.*, **25,** 350–368.
Pirazzoli, P. A., Montaggioni, L. F., Delibrias, G., Faure, G. & Salvat, B., 1985. Late Holocene sea-level changes in the Society Islands and in the northwest Tuamotu atolls, *Proc. Fifth Int. Coral Reef Congr., Tahiti,* **3,** 131–134.
Pirazoli, P. A., Montaggioni, L. F., Vergnaud-Grazzini, C. & Saliege, J. F., 1987. Late Holocene sea levels and coral reef development in Vahitahi Atoll, eastern Tuamotu Islands, Pacific Ocean, *Mar. Geol.*, **76,** 105–116.
Playford, P. E., 1983. Geological research on Rottnest Island, *J.R. Soc. West. Aust.*, **66,** 10–15.
Playford, P. E. & Leech, R. E. J., 1977. Geology and hydrology of Rottnest Island, *Geol. Surv. West. Aust., Report 6.*
Prest, V. K., 1969. Retreat of Wisconsin and recent ice in North America, *Geol. Surv. Canada, Map No. 1257A,* Dept. Energy, Mines and Resources, Canada.
Sabadini, R., Yuen, D. A. & Gasperini, P., 1985. The effects of transient rheology on the interpretation of lower mantle viscosity, *Geophys. Res. Lett.*, **12,** 361–365.
Searle, D. J. & Woods, P. J., 1986. Detailed documentation of a Holocene sea-level record in the Perth region, southern Western Australia, *Quat. Res.*, **26,** 299–308.
Stoddart, D. R., Spencer, T. & Scoffin, T. P., 1985. Reef growth and karst erosion on Mangaia, Cook Islands: A reinterpretation, *Z. Geomorph. N. F., Suppl.* **57,** 121–140.
Stuiver, M., Denton, G. H., Hughes, T. J. & Fastook, J. L., 1981. History of the marine ice sheet in west Antarctica during the last glaciation: a working hypothesis, in *The Last Great Ice Sheets,* eds Denton, G. H. & Hughes, T. J., Wiley, New York.
Thom, B. G. & Roy, P. S., 1983. Sea level change in New South Wales over the past 15,000 years, in *Australian Sea Levels in the Last 15000 Years: A Review,* Monograph Series, Occasional Paper, **3,** pp. 64–85. ed. Hopley, D., Department of Geography, James Cook University of North Queensland.
Thom, B. G. & Roy, P. S., 1985. Relative sea levels and coastal sedimentation in southeast Australia in the Holocene, *J. Sediment. Petrol.*, **55,** 257–264.
van Andel, T. H. & Veevers, J. J., 1967. Morphology and sediments of the Timor Sea, *Bur. Min. Res. Geol. Geophys., Aust., Bull.*, **83,** 1–173.
Veeh, H. H. & Veevers, J. J., 1970. Sea level at −175 m off the Great Barrier Reef 136000 to 17000 years ago, *Nature,* **226,** 536–537.
Walcott, R. I., 1972. Late Quaternary vertical movements in eastern America: quantiative evidence of glacio-isostatic rebound, *Rev. geophys. Space Phys.*, **10,** 849–884.
Walcott, R. I., 1973. Structure of the Earth from glacio-isostatic rebound, in *Annual Review of Earth and Planetary Science,* pp. 15–37, ed. Donath, F. A., Annual Reviews Inc., Palo Alto, California.
Walcott, R. I. 1975. Recent and late Quaternary changes in water level, *Eos, Trans. Am. geophys. Un.*, **56,** 62–72.
Wellman, H. W., 1979. An uplift map for the South Island of New Zealand, and a model for uplift of the Southern Alps, 'The origin of the Southern Alps', *Bull. R. Soc. New Zealand,* **18,** 13–20.

Woodroffe, C. D., Thom, B. G., Chappell, J. & Head, J., 1987. Relative sea level in the South Alligator River region, north Australia, during the Holocene, *Search*, **18**, 198–200.

Woods, P. J. & Searle, D. J., 1983. Radiocarbon dating and Holocene history of the Beacher/Rockingham beach ridge plain, west coast, Western Australia, *Search*, **14**, 44–46.

Wu, P. & Peltier, W. R., 1983. Glacial isostatic adjustment and the free air gravity anomaly as a constraint on deep mantle viscosity, *Geophys. J.R. astr. Soc.*, **74**, 377–449.

Yonekura, N., Matsushima, Y., Maeda, Y. & Kayane, H., 1984. Holocene sea level changes in the southern Cook Islands, in *Sea-level Changes and Tectonics in the Middle Pacific, Rept., HIPAC Project*, pp. 113–133, Krobe University, Japan.

Yuen, D. A., Sabadini, R. C. A., Gasperini, P. & Boschi, E., 1986. On transient rheology and glacial isostasy, *J. geophys. Res.*, **91**, 11420–11438.

APPENDIX 1: DEPTH RESOLUTION OF UPPER MANTLE VISCOSITY PROFILES

The mantle models examined are defined by two parameters, an average viscosity above and an average value below the 670 km discontinuity. Cathles (1975) has argued that a better representation of the structure is a thin (≈75 km), low viscosity (4×10^{19} Pa s^{-1}) channel immediately beneath the lithosphere and overlying a mantle of 10^{21} Pa s^{-1} viscosity. This conclusion was based on an examination of rebound data from sites near the margins of the northern Late Pleistocene ice sheets and from Lake Bonneville. Other studies (Passey 1981; Nakiboglu & Lambeck 1982, 1983) have supported this interpretation but in view of the anomalous tectonic setting of the Lake Bonneville region it is debatable whether the upper mantle in this region is representative of the mantle as a whole. The ability to resolve the detailed rheological structure from observations of rebound at ice-margin sites has previously been questioned on the basis that a very accurate and high-resolution description of the evolution of the ice-load is required and this is generally not available (Nakada & Lambeck 1987, 1988a). Nevertheless, the question as to whether such a thin channel, low viscosity model is representative of the mantle as a whole is important and warrants further examination.

A four-layered mantle model is illustrated in the inset in Fig. A1. The depth of the channel has been fixed by the base of the lithosphere at 50 km and by the depth of 220 km, corresponding approximately to the base of the seismic low velocity layer observed beneath the oceans. Three different values for the viscosity of this channel have been adopted ($\eta_{lvc} = 10^{19}$, 10^{20}, 10^{21} Pa s^{-1}). The predicted sea-level variations during the Late Holocene are generally insensitive to the introduction of the low-viscosity channel (Fig. A1), particularly at the continental margin sites where

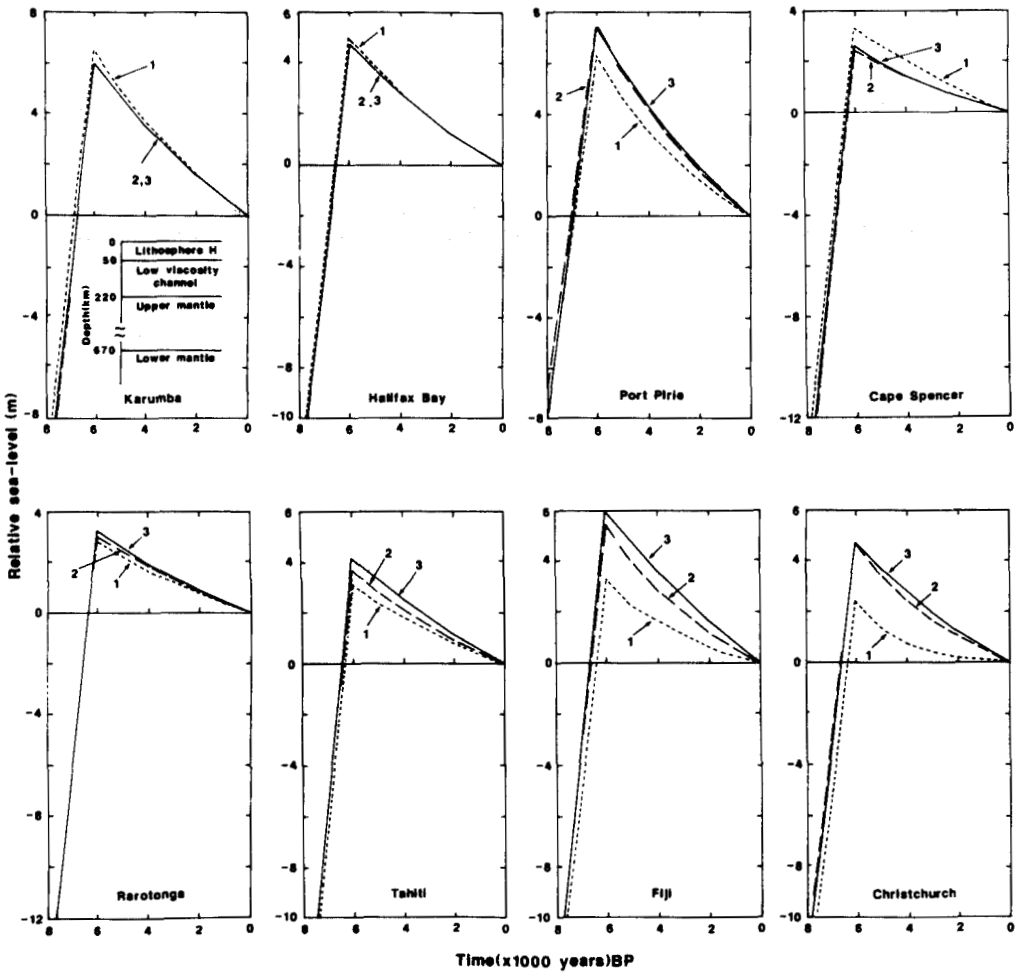

Figure A1. Relative sea-level curves for the ice models ARC 3 + ANT 3, lithospheric thickness $H = 50$ km, lower mantle viscosity 10^{22} Pa s^{-1}, upper mantle viscosity of 10^{21} Pa s^{-1} and a low viscosity channel of (1) 10^{19} Pa s^{-1}, (2) 10^{20} Pa s^{-1}, (3) 10^{21} Pa s^{-1}.

the effective wavelength of the water load is of the order of the scale of the continent. Only at sites such as Port Pirie where the length-scale of the Late Holocene meltwater load is characterized by the dimensions of the gulf, does the response become dependent on the detailed viscosity structure by amounts of about 10–15 per cent for a two-order-of-magnitude reduction in η_{lvc}.

At islands, the sensitivity of the crustal response to the presence of a low viscosity channel is governed by the length scales of the island and the ocean basin. For very small islands it is the latter that controls this response and sea-levels at these sites will be insensitive to the presence of such a channel (Fig. A1). At large islands, such as Fiji or the South Island of New Zealand, where the island size is similar to the depth to the base of the channel, the sea-level response is more sensitive to such a channel, provided that the viscosity reduction is by more than an order of magnitude and provided that the lithospheric thickness is known.